DEVELOPMENT OF A SIMPLE DIAGNOSIS TOOL FOR DETECTING LOCALIZED ROUGHNESS FEATURES

Karim Chatti, Ph.D.
Imen Zaabar, M.S.
Hyung Suk Lee, M.S.

Michigan State University

Department of Civil and Environmental Engineering
Pavement Research Center of Excellence

Final Report
Project RC-1505

February 2009

Technical Report Documentation Page

1. Report No. RC-1505	**2. Government Accession No.**	**3. MDOT Project Manager** Mike Eacker
4. Title and Subtitle Development Of A Simple Diagnosis Tool For Detecting Localized Roughness Features		**5. Report Date** February, 2009 **6. Performing Organization Code**
7. Author(s) Karim Chatti, Associate professor Imen Zaabar, Graduate Research assistant		**8. Performing Org. Report No.**
9. Performing Organization Name and Address Pavement Research Center of Excellence Michigan State University Department of Civil and Environmental Engineering, 3546 Engineering Building, Michigan State University East Lansing, MI 48824-1226		**10. Work Unit No. (TRAIS)** **11. Contract No.** **11(a). Authorization No.**
12. Sponsoring Agency Name and Address Michigan Department of Transportation Construction and Technology Division P.O. Box 30049 Lansing, MI 48909		**13. Type of Report & Period Covered** Final Report **14. Sponsoring Agency Code**

15. Supplementary Notes
This project corresponds to Task B of the project Effect Of Michigan Multi-Axle Trucks On Pavement Distress and Profile.

16. Abstract
The collection of distress data from video imaging of the pavement surface can provide the location and type of many distresses. However, it cannot provide useful information about some distress features such as the magnitude of faulting, breaks and curling in concrete pavements. This report describes a simple tool to extract such information through the use of the raw profile data. Different methods were used in the study, including wavelets, time frequency and discrete methods. The discrete elevation difference method (DED) was selected for faulting and breaks detection, and the discrete slope method (DS) was selected for curling detection. To test the validity of the analysis, surveys were conducted on different sites in Michigan. The new tool was able to detect the magnitude of faulting, breaks and curling with an R^2 of 0.97 and standard error (SE) of 0.25 mm. The localization was also highly accurate (R^2 =0.99). The results indicate that the methods described above can capture relevant information about these roughness features with reasonable accuracy.

17. Key Words Detection, Localized roughness features, Faulting, Breaks, Curling	**18. Distribution Statement** No restrictions. This document is available to the public through the Michigan Department of Transportation.

19. Security Classification - report	**20. Security Classification - page**	**21. No. of Pages**	**22. Price**
Unclassified	Unclassified	74	

TABLE OF CONTENTS

LIST OF FIGURES

LIST OF TABLES

CHAPTER 1
INTRODUCTION

1.1 BACKGROUND

Michigan's PMS system collects pavement surface distresses (type, extent, and severity) from video images of the pavement surface bi-annually. The raw profile is measured by a high speed profilometer. Surface distresses and profile data are used to compute Distress Index (DI) and Ride Quality Index (RQI), for a minimum segment length of 0.1 mile. The bi-annual change of the pavement's DI is included in a performance model to estimate the pavement's Remaining Service Life (RSL).

Road roughness indices such as the International Roughness Index (IRI) and RQI are useful as indicators of the level of pavement serviceability. Each of these summary roughness statistics offers a convenient index for monitoring the trend of pavement roughness deterioration with time. However, they do not retain the actual contents of pavement surface roughness. Such detailed roughness information may be useful for maintenance operations, and detection of roughness features. The collection of distress data from video images of the pavement surface can provide the location and type of many distresses. However, because video images of pavement surface are two-dimensional, they cannot quantify pavement surface characteristics. Therefore, such images cannot provide useful information about roughness features, such as their magnitude. Failure to include specific roughness features in Pavement Management Systems (PMS) has the following negative impacts on system performance:

(1) The analysis may overestimate the RSL of the pavement;
(2) The system process may not select the most appropriate fix to extend pavement life.

1.2 RESEARCH OBJECTIVES

The objectives of this research study are:

1. Developing a profile-based diagnosis method for distinguishing non-identifiable surface distresses from video imaging that have one of the following impacts:
   a) Significant impact on pavement structural integrity
   b) Significant impact on pavement roughness, as determined from RQI
   c) Significant cause of pavement deterioration

2. Developing a window-based software system that can detect the presence of certain distresses from the profile and then tabulate these distresses, as identified in objective (1).

1.3 ORGANIZATION

This final report contains 3 chapters including this introductory chapter. Chapter 2 investigates methods of identifying certain pavement distresses through the use of profile data. Finally, Chapter 3 presents the user's manual for the new profile-based diagnostic tool for identifying surface distresses.

CHAPTER 2
PAVEMENT DISTRESS AND ROUGHNESS IDENTIFICATION

2.1 INTRODUCTION

MDOT annually collects the distress and profile data in order to calculate the Distress Index (DI) and Ride Quality Index (RQI). The distress data from the video imaging of the pavement surface may provide where certain distresses are present. However, some information about the distress such as the magnitude of faulting or curling can not be extracted from the two dimensional video images. The objective of this analysis presented in this chapter is to extrapolate such information through the use of the profile database.

2.2 LITERATURE REVIEW

Although a lot of information on profile analyses is documented, they are mostly based on an index type (i.e. IRI, RQI, etc.) of analyses. Few studies were found under the subject of diagnosing/localizing distresses from the actual profile data.

De Pont (1999) introduced wavelets to be used for identifying the local features of the profile. The method he suggested localizes the features of the profile in terms of short, medium and long wavelengths. However, the method does not identify the individual distresses that are present. De Pont also discussed the usefulness of the wavelets in terms of compressing the profile data for storage. From his example, the profile data was compressed into only 5% of the size of the original signal, and the reconstructed signal had a maximum difference of 0.003m (0.12 in) in comparison to the original signal.

Byrum (2001) developed an algorithm that picks up the “imperfection” zone from the profile of rigid pavements. These imperfection zones are then separated from the slab region, and then the curvature index is calculated for the slab region. The identification of the imperfection zone is done by calculating the curvature of the profile and applying a threshold on the curvature. The curvature variation threshold (CVT) is calculated by the following equation:

$$CVT = 1/12\left[-0.0213 + 0.03242(06CVStDev)^{0.8405} + 0.00665(24CVStDev)^{1.1446} - 0.06631(48CVStDev)^{3.7819}\right]$$

$(0.003 < CVT < 0.015\ ft^{-1})$
$R^2 = 0.81$

Where: 06CVStDev = Standard deviation of the 6″ curvatures in 500 ft. profile, 1/ft *1000

24CVStDev = Standard deviation of the 24″ curvatures in 500 ft. profile, 1/ft *1000

48CVStDev = Standard deviation of the 48 ″ curvatures in 500 ft. profile, 1/ft *1000

Fernando and Bertrand (2002) used moving average filters to detect localized roughness. The points where the deviations from the averaged profile are large are the rough areas. However, this method does not identify the actual distresses.

Attoh-Okine (2003) introduced wavelet analysis as a method of profile analysis. He mentions that using wavelet analysis; the profile may be studied beyond the index type of analyses.

Chang et al. (2005) identified localized roughness based on the Texas Department of Transportation Specification Tex-1001-S. First, each elevation point from the two longitudinal profiles (left and right wheel paths) is averaged to produce a single averaged wheel path profile. Then, the resulted profile is placed on a 7.6 m (25 ft), centered-moving average filter. The difference between the average wheel path profile and the 7.6m-moving average filtered profile for every profile point is computed. Deviations greater than 3.8 mm (0.15 in) are considered a detected area of localized roughness. Positive deviations are considered as "bumps" and negative ones as "dips". However, this method does not identify the distress type.

2.3 REVIEWING MDOT'S DATA SOURCE

MDOT's current contractor for video and laser data collection is Pathway Services Inc. The Pathway laser profiler collects the elevation of the profile at every 0.75 inches (the sampling interval). These measurements are averaged every 3 inches and recorded (the recording interval). These profile samples are taken for left and right wheel paths and the center of the lane. For each of the longitudinal profiles, the differences in height 3 inches apart are taken and the variance of the differences of the heights is calculated for each point. Then, a moving average filter is applied to the calculated variances and compared with the actual elevation differences. The base length for the variance and moving average calculations is 20 ft (10 ft before and after). This procedure is repeated for all three longitudinal profiles (left and right wheel paths and the center of the lane), and if the elevation difference is greater than the averaged variance for all three longitudinal profiles, then the point is classified as faulting. Figure 2.1 shows a dummy profile generated by the research team (see section 2.4 for details of the dummy profile) and the faulting detected by the Pathway's procedure. Note that this is only for a single longitudinal profile. The procedure detects the presence of faulting but in a wide range rather than at a certain point.

The research team was able to access the profiles that were collected by MDOT during 1993-99. These profiles were collected with a sample interval of 3 in, which is the interval still in use by MDOT. However, the sections corresponding to the profiles do not provide the research team with the distress locations.

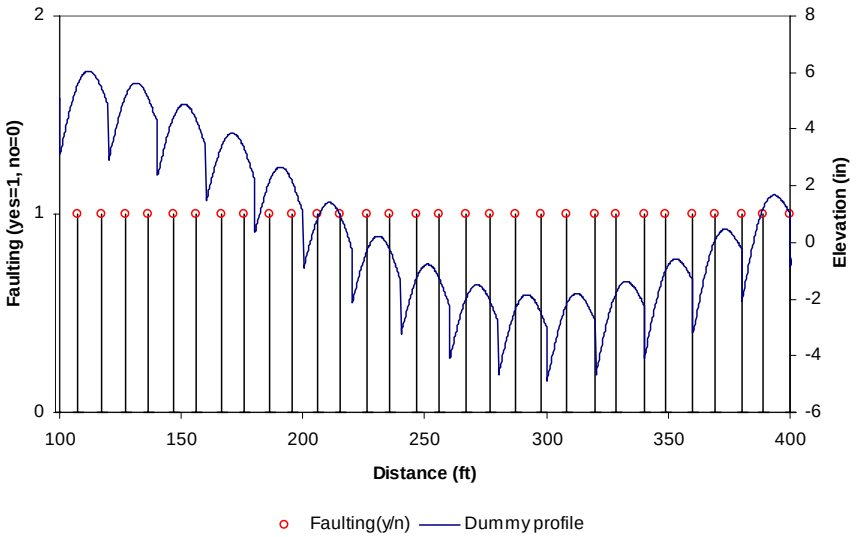

Figure 2.1 Faulting detected by Pathway's procedure

Meanwhile, the research team had used the profile and distress data from LTPP SPS-2 sections including a few sections in Michigan. These data were extracted from the LTPP database. The profiles were collected using a sample interval of 1 in. Prior to being entered into the database, the collected samples are passed through a 300 ft high-pass filter to eliminate the gradual, long wavelengths. After that, the profiles are reported with a sample interval of 6 in. The distresses such as faulting of LTPP sections can be identified from the database. However, the database does not contain information about curling of rigid pavement slabs.

2.4 EVALUATING OTHER METHODS FOR ANALYZING A PROFILE

Since the research team did not have access to the recent (at the time of this project) profile data collected by the Pathway profilometer, old profiles collected by MDOT during 1993-1999 and the LTPP profiles were studied.

2.4.1 Pavement Faulting

Faulting and curling of slabs are the major rigid pavement distresses that need to be identified from a surface profile because they cannot be determined from video imaging. Faulting of the joints/cracks is defined as the difference in elevation of the two adjacent slabs before and after the joint/crack, as shown in Figure 2.2. Theoretically, when the samples of the profile are collected over a faulted joint/crack, the difference in elevation should appear in two adjacent samples. However, from the MDOT profile data the faulting does not appear in two adjacent points. Faulting of the slabs in the actual

profile appears at several sample points, as shown in Figure 2.3. Thus, the best way to evaluate faulting is that the differences in elevation be taken from the raw profile before applying the moving average filter. Another way will be explained later.

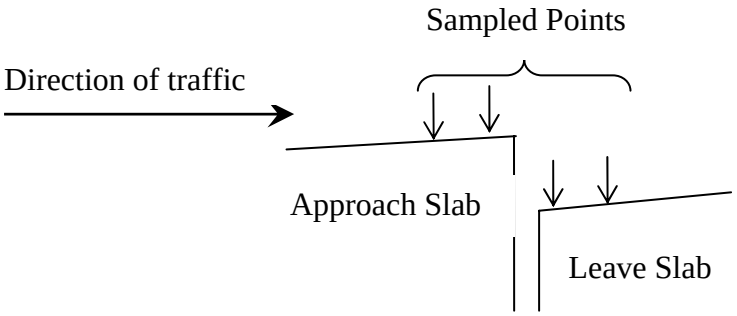

Figure 2.2 Theoretical samples from faulting of slabs

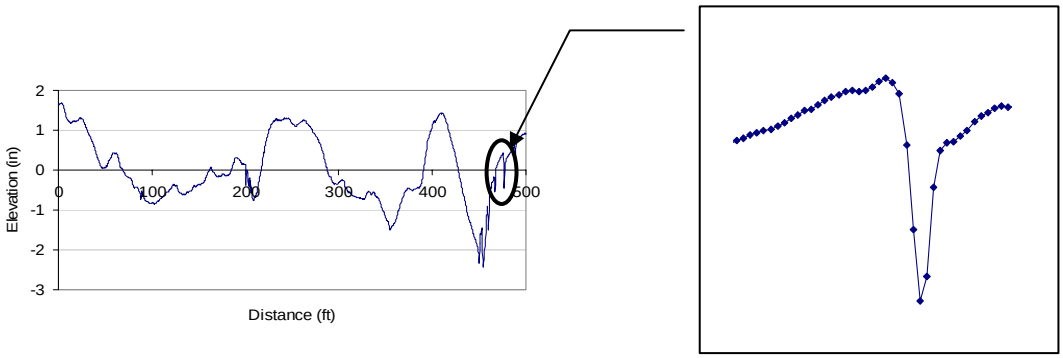

Figure 2.3 Faulting from actual profile

In order to explain such phenomenon, the research team performed a study using a dummy profile. The dummy profile was created to include the following:

- Long wave sinusoid that represents the topography of the site.
- Short wave sinusoid that represents the curling of the slabs.
- Discontinuous line that represents the faulting of the joints/cracks.

Figure 2.4 shows the components of the dummy profile listed above. The dummy profile is the sum of these three functions and is shown in Figure 2.5. A sample interval of 3 inches was used to meet the current sampling interval used by MDOT.

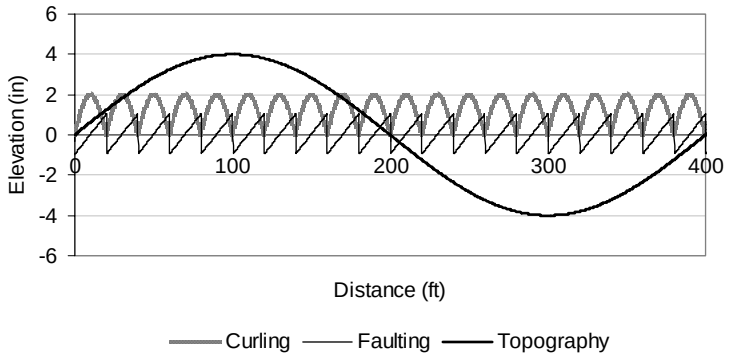

Figure 2.4 Components of the created dummy profile

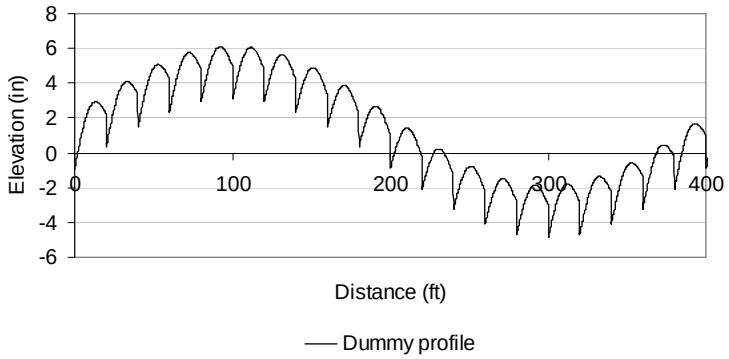

Figure 2.5 Dummy profile

In the dummy profile, faulting was created by a significant difference in elevation of the adjacent samples as shown in Figure 2.6. Also shown in the figure is a profile with faulting that is similar to the actual profile data (faulting appears within several sample points). This profile was obtained by passing the dummy profile through a moving average filter with a base length of 1 ft.

The moving average filter is a low-pass filter that smoothes the profile and is a built-in filter of the profilometer in most cases. The number of sample points to show a faulting is highly affected by the type of the low-pass filter and its base length. However, the research team had no access to the raw profile at that time which would be very useful to determine the moving average filter base length.

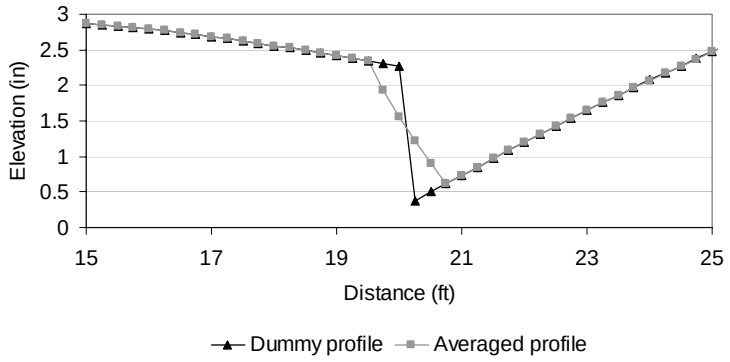

Figure 2.6 Faulting of dummy profile

2.4.1.1 Methods for Identifying Joint/Crack Faulting

Four methods were studied for identifying the faulting from a profile; (1) Discrete Elevation Difference (DED) method, (2) Discrete Slope (DS) method, (3) Discrete Curvature (DC) method and (4) Wavelet analysis method. The DED method takes the elevation difference of the two discrete sample points. These two points would be the two adjacent points if there were no filters applied to the profile that is being analyzed. However, because the faulting appears in several points in a filtered profile, the two points are not adjacent but exist with some distance apart. This distance would be dependent on the type and the base length of the filter applied to the profile.

The DS method is used to detect discontinuities in digital image processing. It is similar to the DED method in the sense that it takes the difference of the elevation heights. But the difference is that the slope (difference in elevation) is taken from the adjacent sample points. The DC method is similar to the DS method other than that it takes the curvature (2^{nd} derivative) of the profile.

Wavelet analysis is a popular method for compression and multi-resolution analysis of discrete signals. It decomposes a given signal into several signals of different scale. The term ‘scale’ here is related to frequency. Thus, it allows the user to see the signal in different scales along with time or distance.

However, all the analyses herein are based on the averaged profile and not the raw profile except for the artificially generated dummy profile. It is again because the research team did not have the raw profile data at that time.

Figure 2.7 shows an example of the wavelet analysis of a profile from LTPP section (20-0201). “D1” and “D2” may be treated as noise since they are decomposed of high frequency contents. “D3” and “D4” may provide useful information depending on the type of the mother wavelet used. The highlighted locations in Figure 2.7 might have potential of faulting or cracking since they show high variations in the decomposed signal.

The wavelets used were haar wavelets, daubechies (db) wavelets, symlets (sym), and coiflets (coif).

Once the method is decided, then it is important to decide on the threshold. Two possible methods are suggested: (1) Threshold, and (2) Adaptive Filtering. Thresholds may simply be applied on the slope, curvature, DED, and on wavelets. Figure 2.8 shows an example of threshold applied on the slope with a value of 0.3. With this threshold, all the locations that have slopes in between -0.3 and 0.3 are considered to be continuous. Although it is not shown in figures 2.9 and 2.10, similar thresholds may be applied to the curvature and DED. Unlike the example of threshold shown in figure 2.7, deciding on a threshold value is not a simple problem. Sufficient profile data was needed to decide on a reliable threshold.

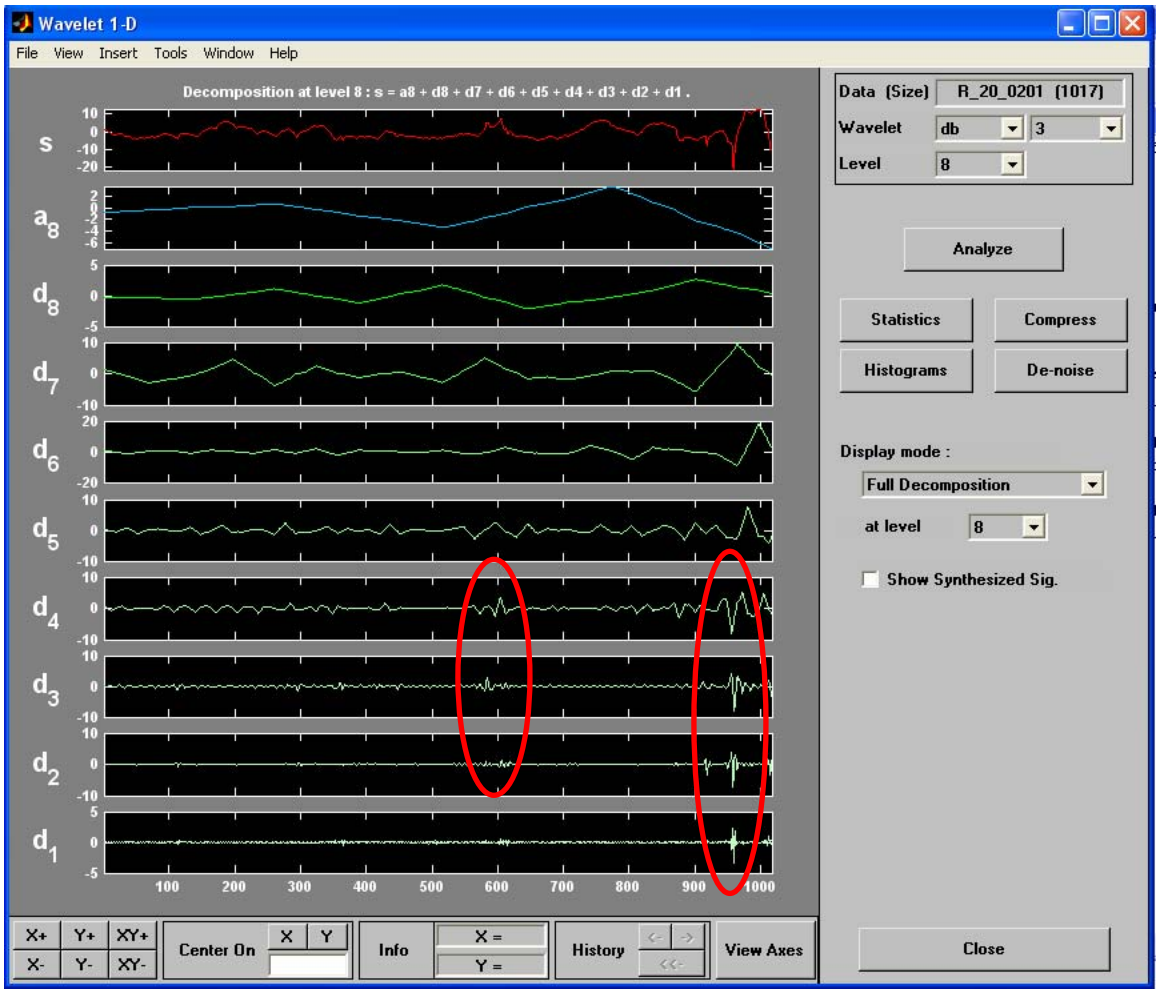

Figure 2.7 Daubechies 3 wavelet analysis

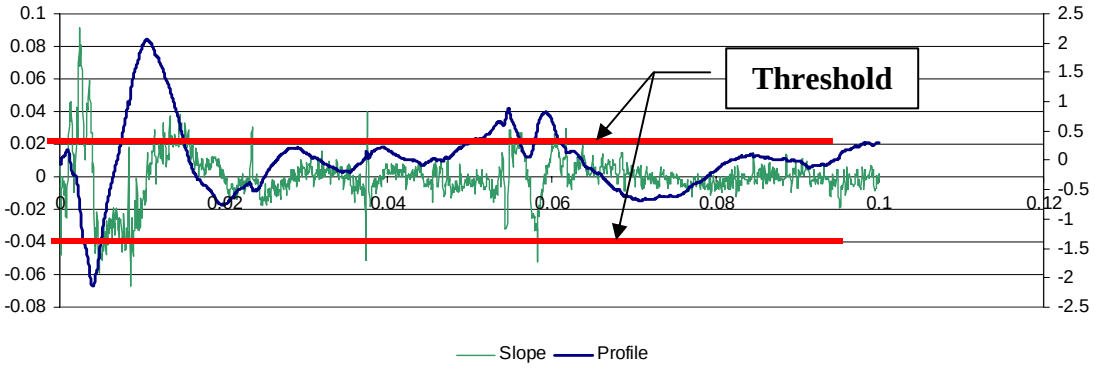

Figure 2.8 Profile and slope

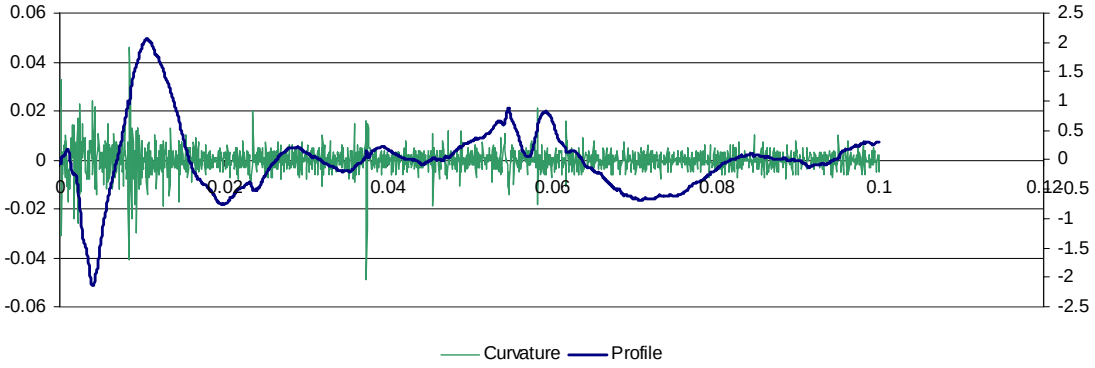

Figure 2.9 Profile and curvature

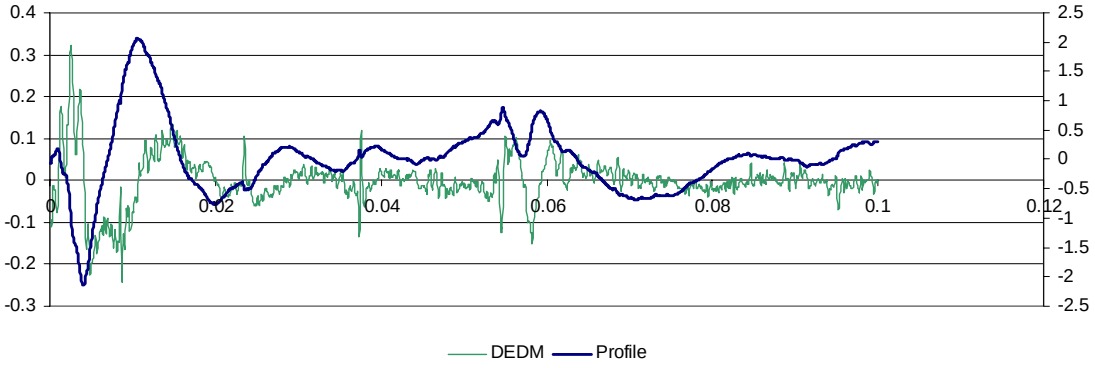

Figure 2.10 Profile and discrete elevation difference

Adaptive filtering is a method used in digital image processing. It calculates the global and local standard deviation and compares with each other. If the global standard deviation (GSTD) is greater than the local standard deviation (LSTD) around a point, then that point in the sample is continuous. If the LSTD is greater than the GSTD, then the point around where the LSTD is calculated is not continuous. Thus, the GSTD of a given sample acts like a threshold. The advantage of this method is that given the samples, the threshold (GSTD) is easily calculated. However, the inherent disadvantage is that the

threshold is dependent on the number of sampled points and if the signal is very noisy it does not clearly point out the locations of discontinuities (figure 2.12). Figures 2.11 through 2.13 show the discontinuities on the profile using the slope, curvature and DEDM, respectively, along with the adaptive filtering.

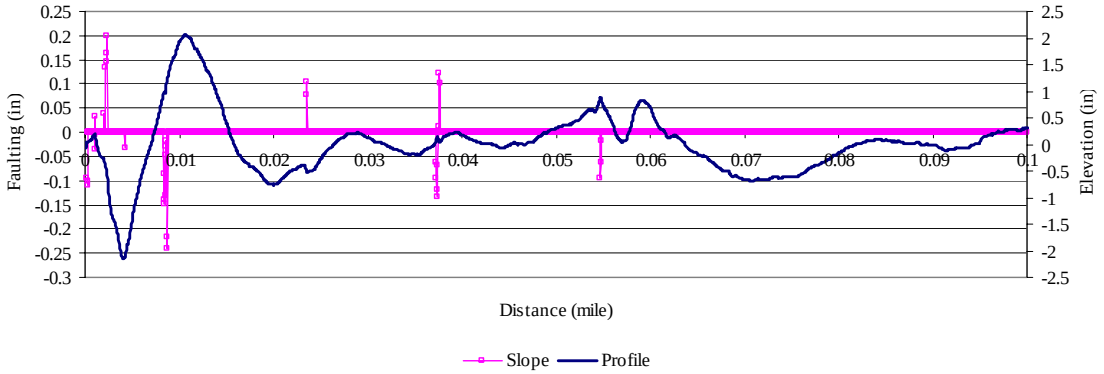

Figure 2.11 Discontinuities detected by slope and adaptive filtering

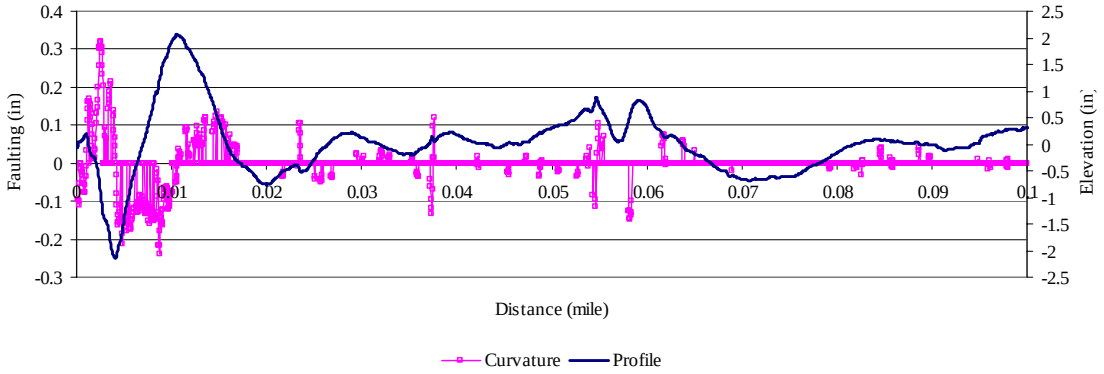

Figure 2.12 Discontinuities detected by curvature and adaptive filtering

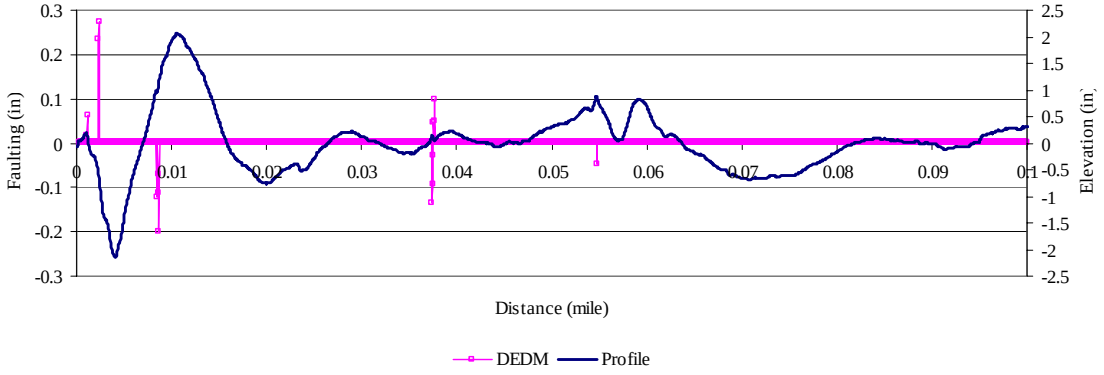

Figure 2.13 Discontinuities detected by discrete elevation difference and adaptive filtering

The methods mentioned above were tested using LTPP profile data. The LTPP section with the highest faulting (14 mm) was selected.

Figures 2.14 through 2.19 show a profile of an LTPP section with faulting that was measured from the field with an accuracy of ±1 mm. The figures also show the faultings that were detected from the methods described above and a threshold value of 1 mm for DEDM and slope method while 0.5 mm was used for D1's of wavelets. Figures 2.20 through 2.25 show the same methods but with adaptive filtering instead of the threshold. The discrete elevation difference method detected the faulting better than the wavelet methods in terms of location and magnitude.

2.4.1.2 Discrete Elevation Difference method with threshold

For the reasons mentioned above, the research team has selected the DED method with threshold for detecting faulting at joint/crack. To summarize, the discrete elevation difference method consists of computing the difference in elevation between points at a given interval. Theoretically, when the samples of the profile are collected over a faulted joint/crack, the difference in elevation should appear in two adjacent samples. However, as shown before, the faulting of the slab in the raw profile appears at several sample points (Figure 2.6). As seen before, the elevation is collected at every 0.75 in [sampling interval] and recorded at every 3 in [recording interval]. Consequently, when the difference in elevation is computed, each fault/crack is represented by a range of differences. Thus, the largest absolute value (local maximum) for each range of differences was taken as the fault magnitude (Figure 2.26). However, as it can be seen from figure 2.27, if the faulting is calculated based on the elevation difference of adjacent points, three different values of the fault magnitude can be obtained, depending on whether the distance to the fault is a multiple of the recording interval:

(1) Exact magnitude, [Figure 3 (a)];
(2) 75% of the exact magnitude, [Figure 3 (b) and (d)];
(3) 50% of the exact magnitude [Figure 3 (c)].

In order to resolve this problem, it was decided to take the difference in elevation between the points that are 6 in apart (±3 in. of the point of interest). The algorithm for the fault detection method is described in Figure 2.28.

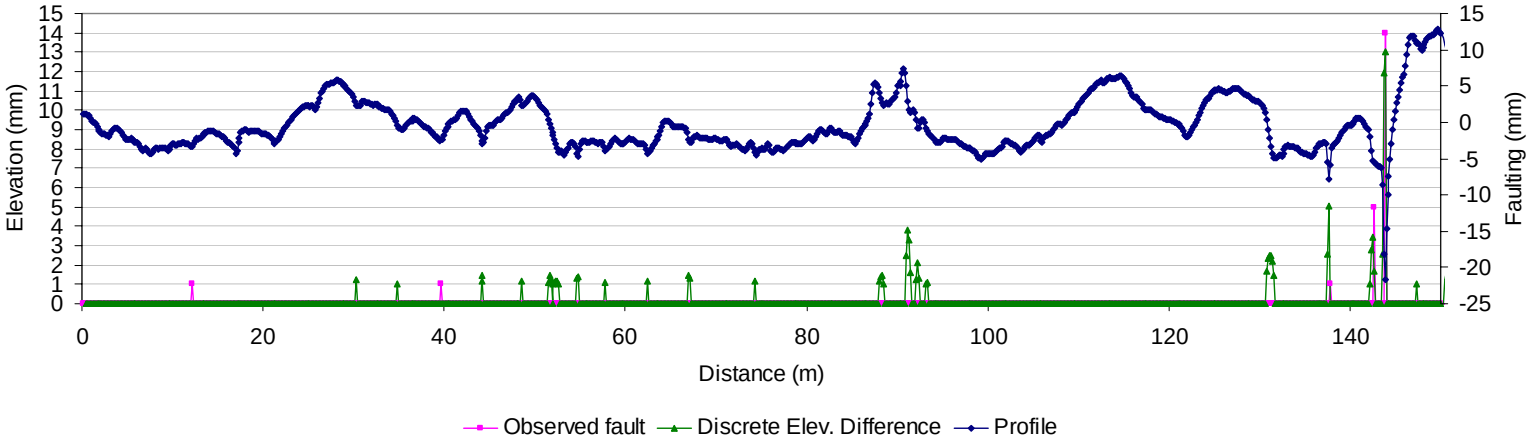

Figure 2.14 Detected faulting from the discrete elevation difference method

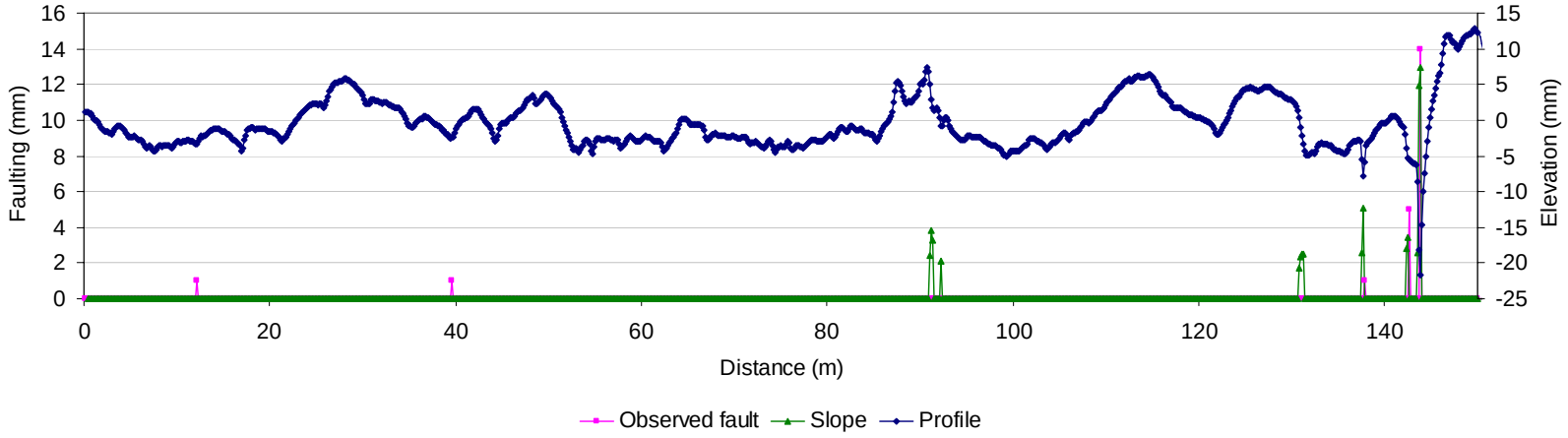

Figure 2.15 Detected faulting from the slope method

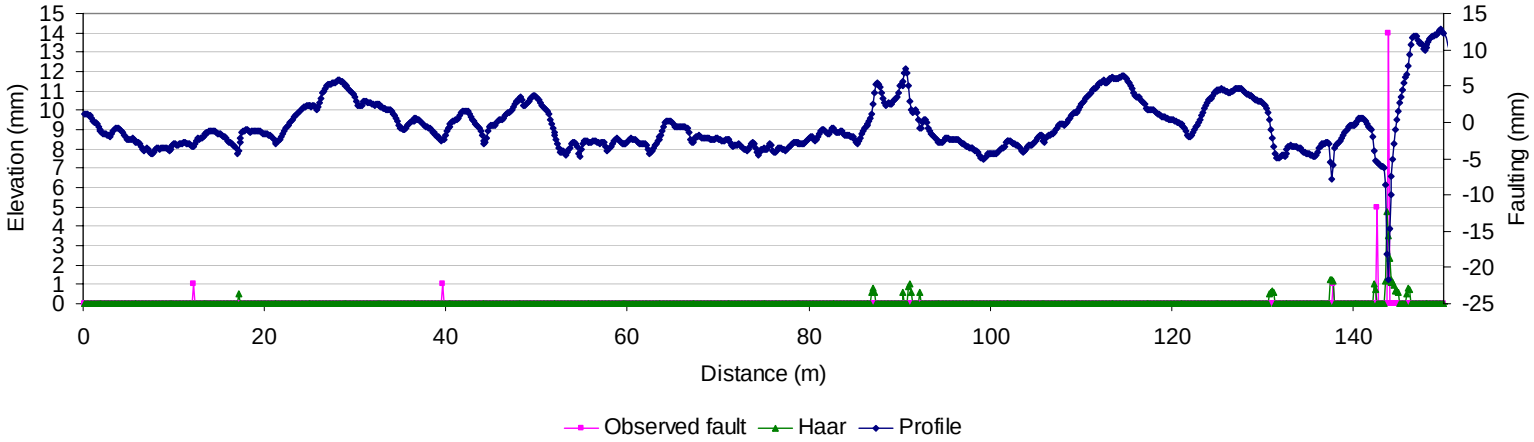

Figure 2.16 Detected faulting from the Haar wavelet method

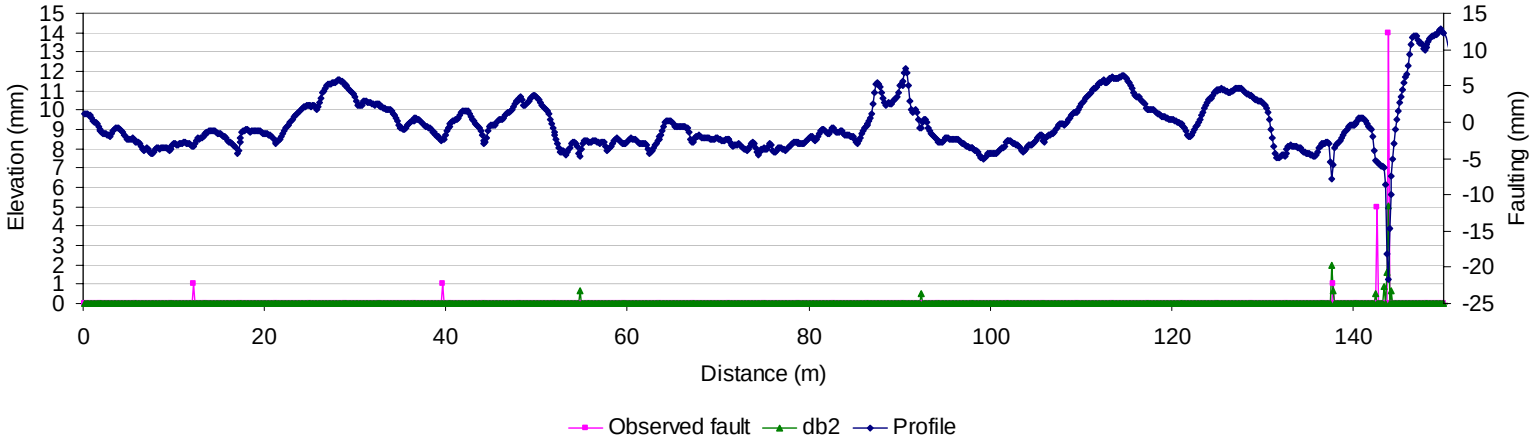

Figure 2.17 Detected faulting from the db2 wavelet method

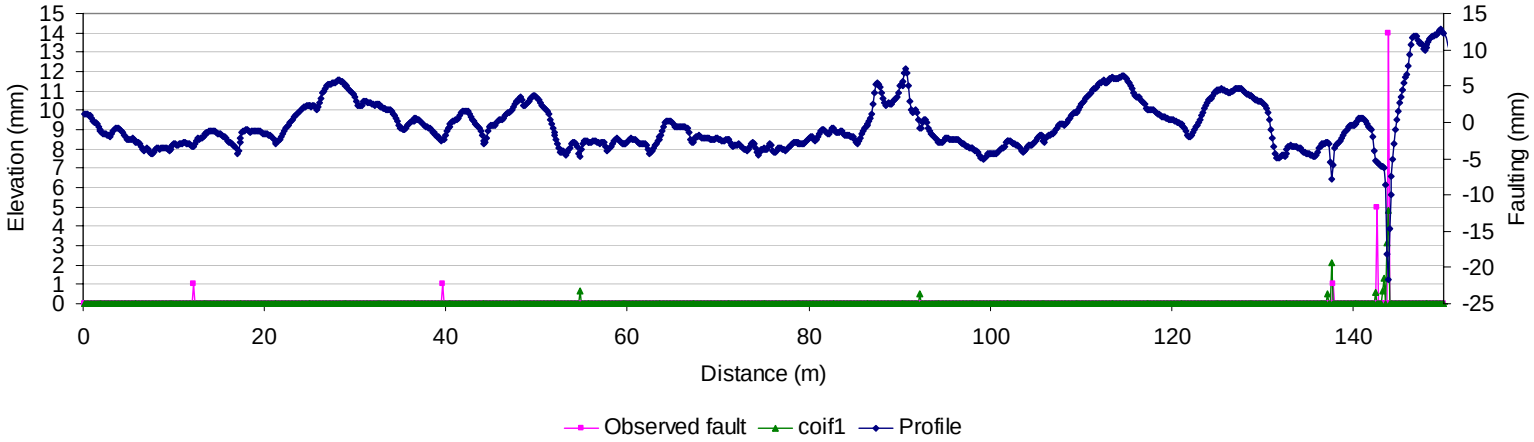

Figure 2.18 Detected faulting from the coif1 wavelet method

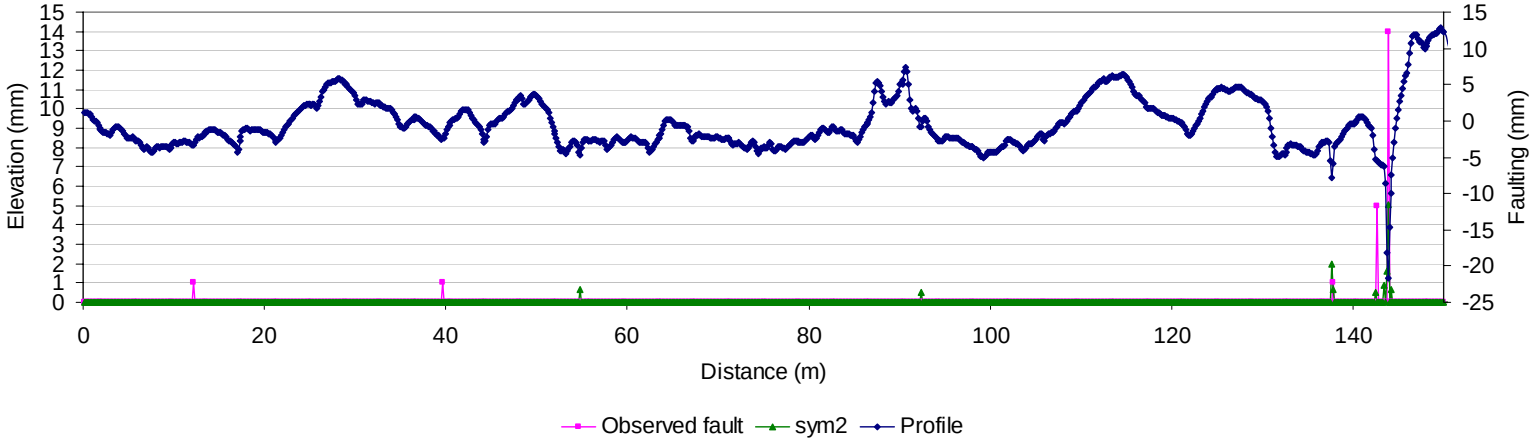

Figure 2.19 Detected faulting from the sym2 wavelet method

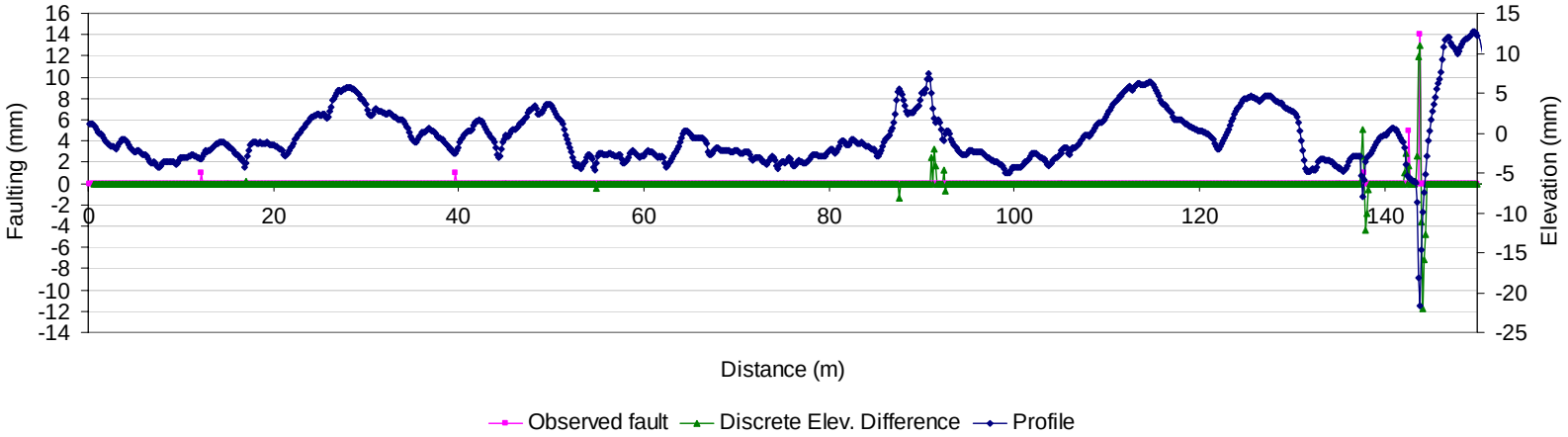

Figure 2.20 Detected faulting from the discrete elevation difference method & adaptive filtering

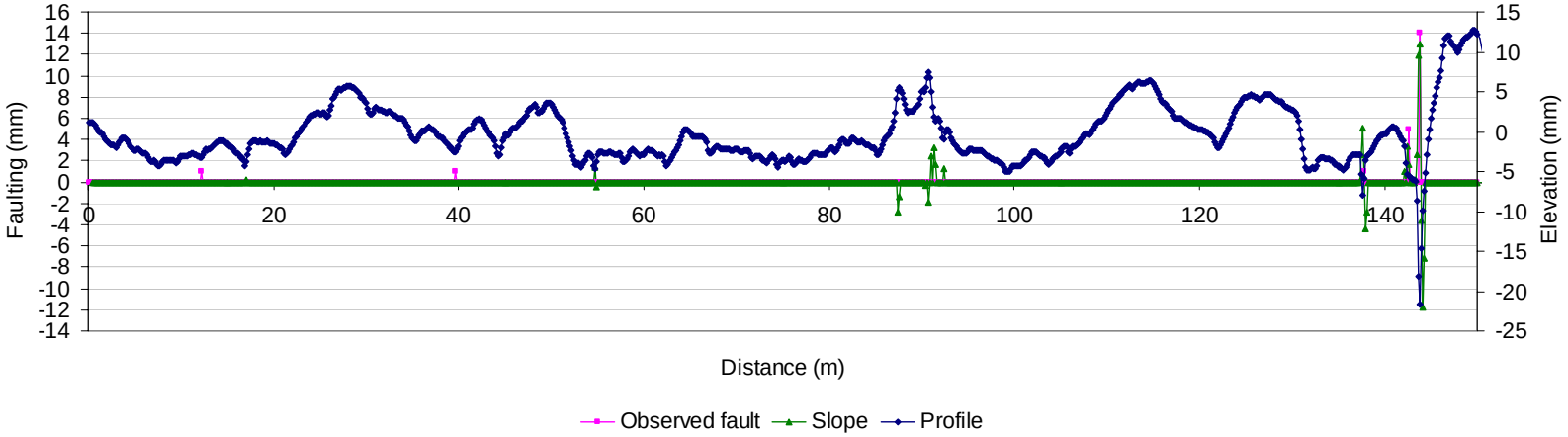

Figure 2.21 Detected faulting from the slope method & adaptive filtering

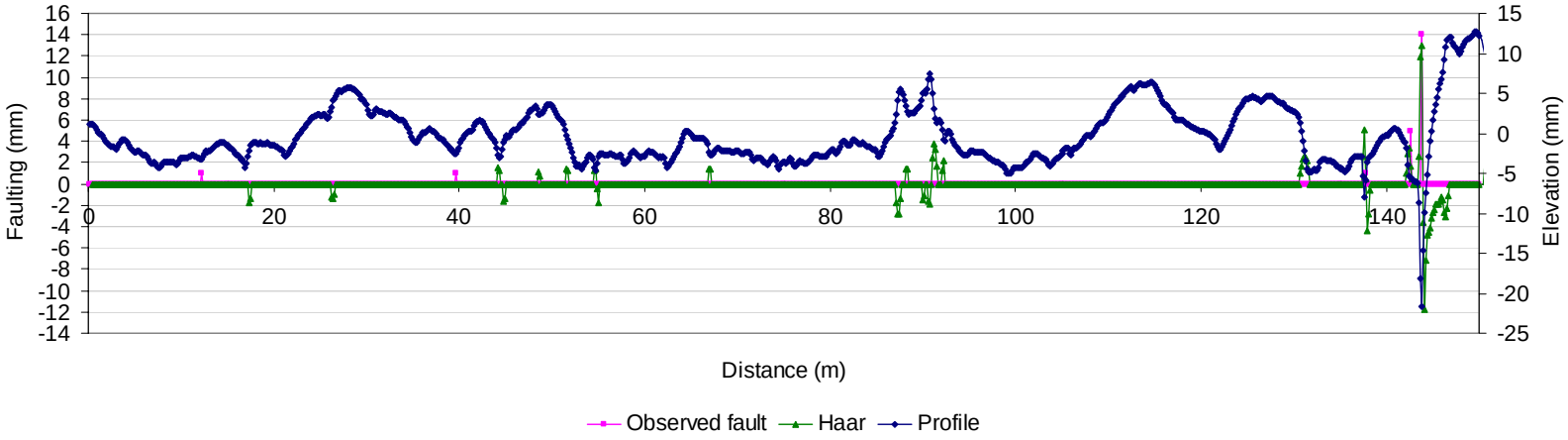

Figure 2.22 Detected faulting from the Haar wavelet method & adaptive filtering

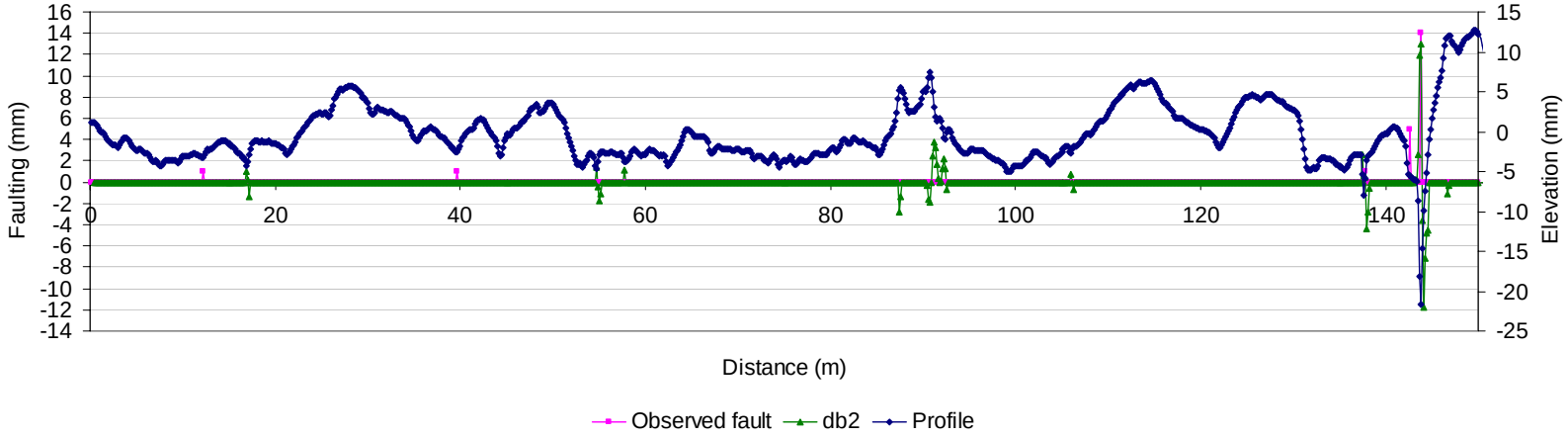

Figure 2.23 Detected faulting from the db2 wavelet method & adaptive filtering

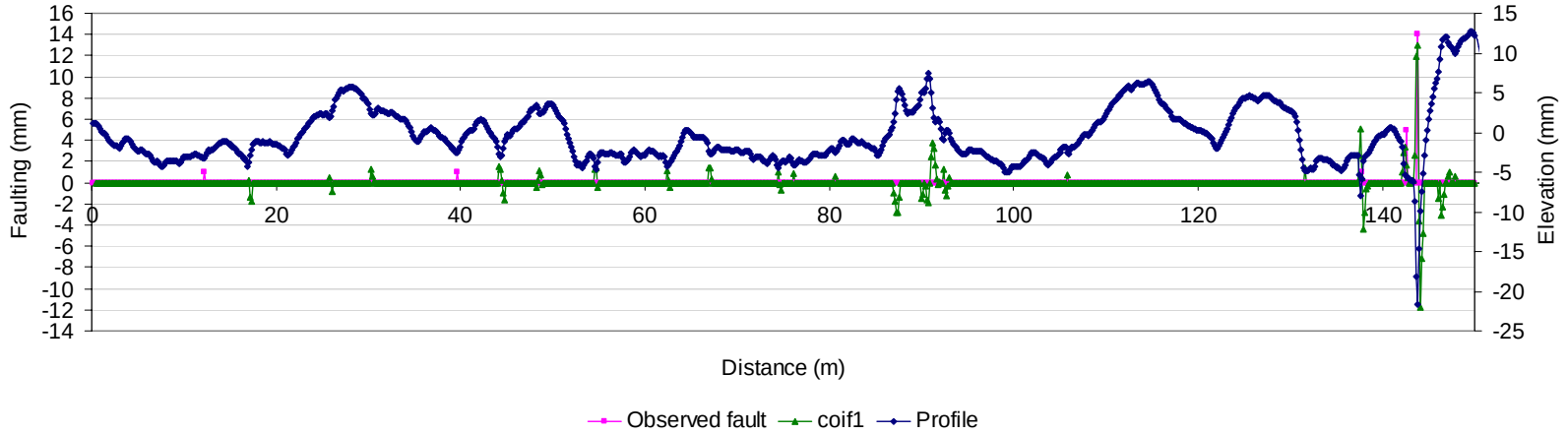

Figure 2.24 Detected faulting from the coif1 wavelet method & adaptive filtering

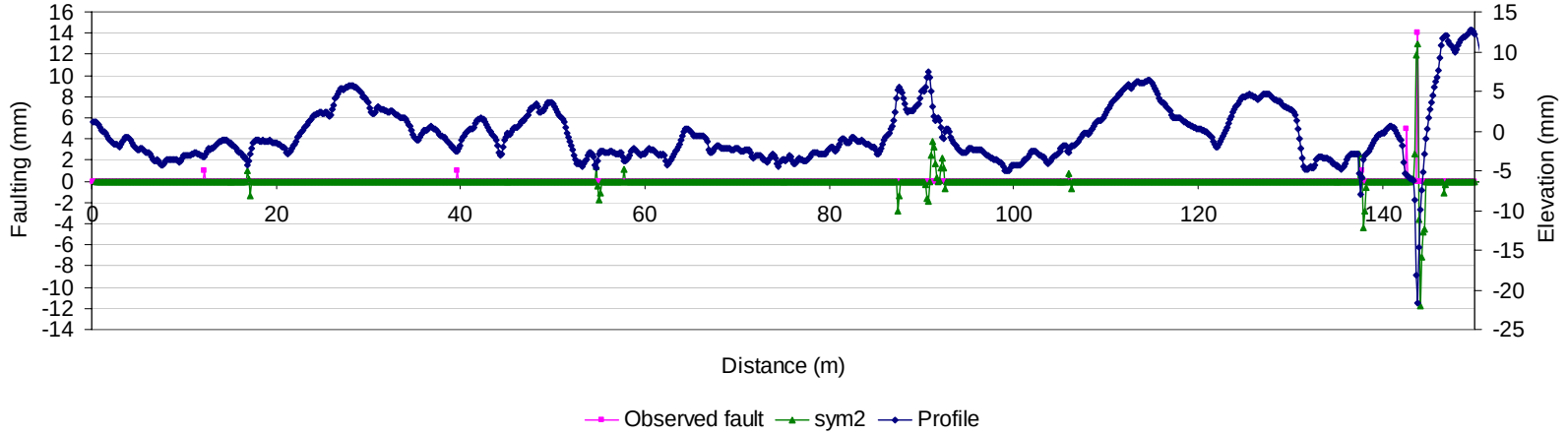

Figure 2.25 Detected faulting from the sym2 wavelet method & adaptive filtering

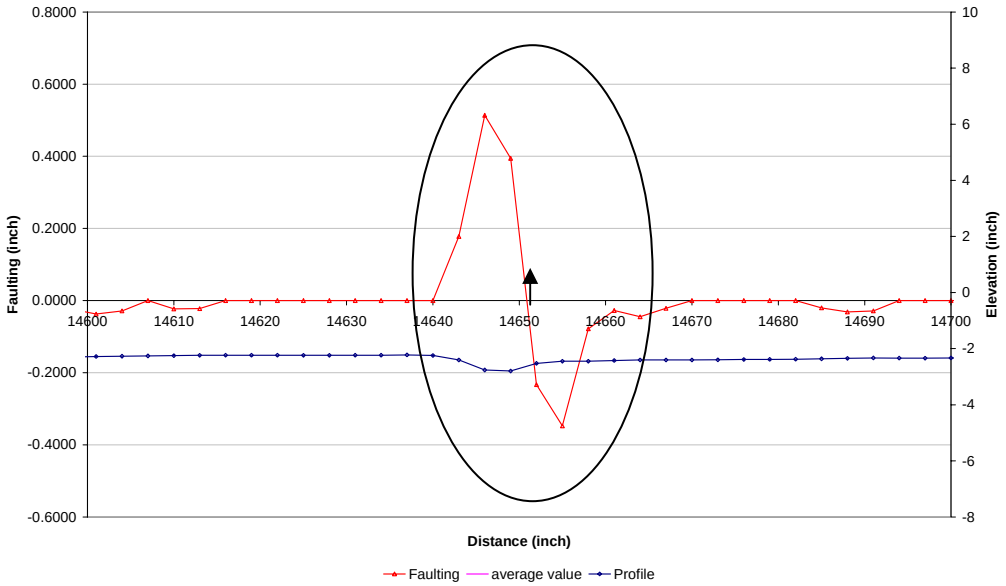

Figure 2.26 Faulting at a crack and its maximum value

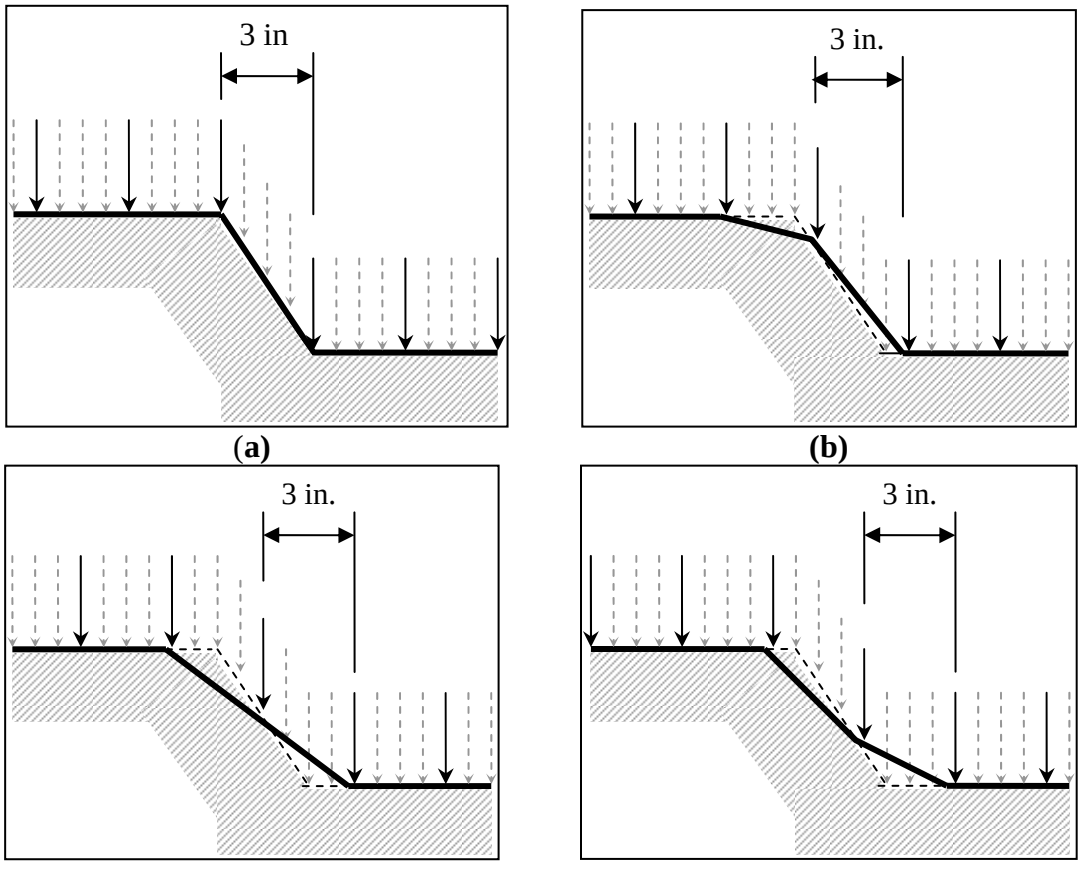

Figure 2.27 Different scenarios of recording a fault after filtering

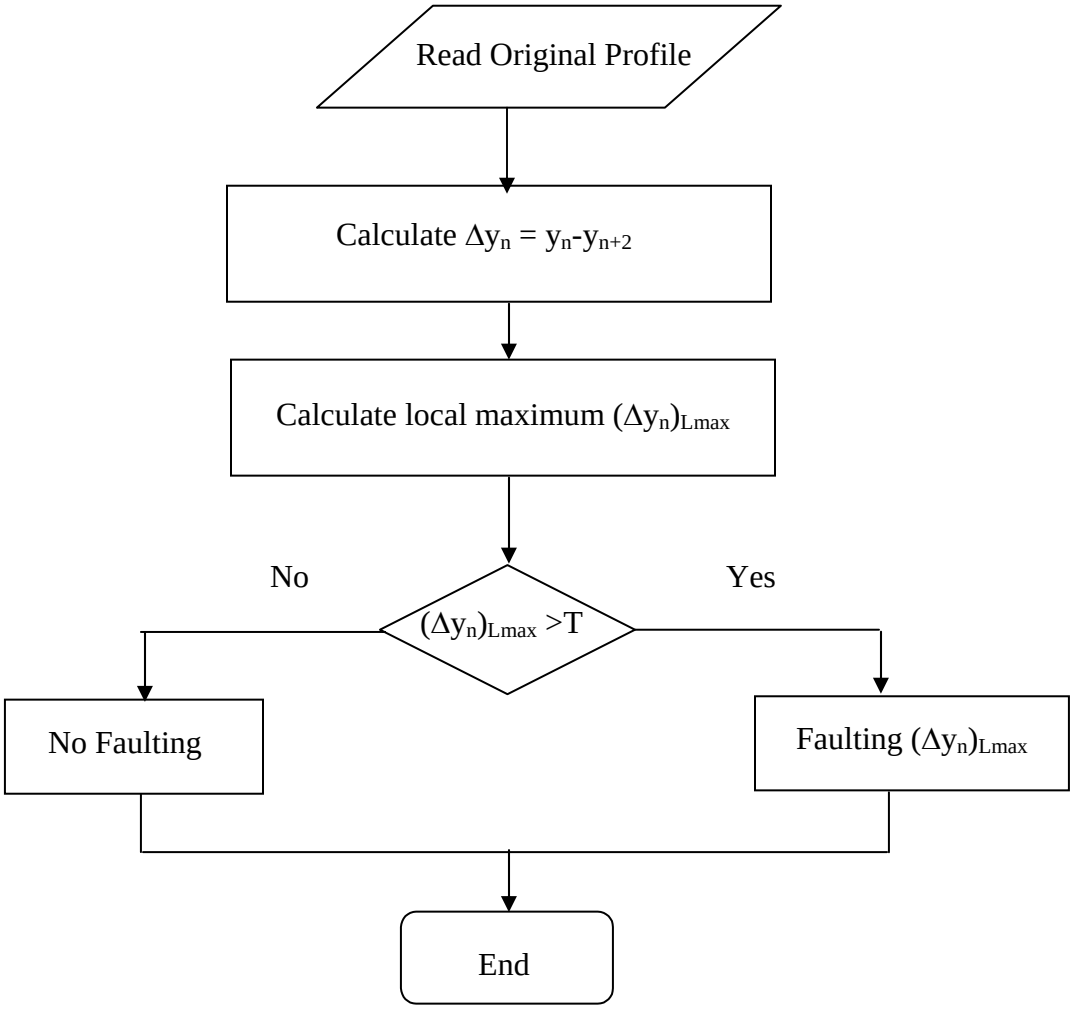

Figure 2.28 Fault detection algorithm

2.4.2 Pavement Breaks

A pavement break is a broken portion of the pavement section that starts with a negative fault and ends with a positive fault. The research team has decided that the distance between the two opposite faults should not exceed 3ft (Figure 2.29). This threshold could be updated according to MDOT needs.

Before detecting breaks, different steps are followed. First, differences in elevation are computed. This step is the same as the fault detection method. Second, if the sign of two successive faults is different, the method checks the distance between them: if the distance is less than 3ft, it is considered break; otherwise, there is no break. The algorithm for the breaks detection is described in Figure 2.30.

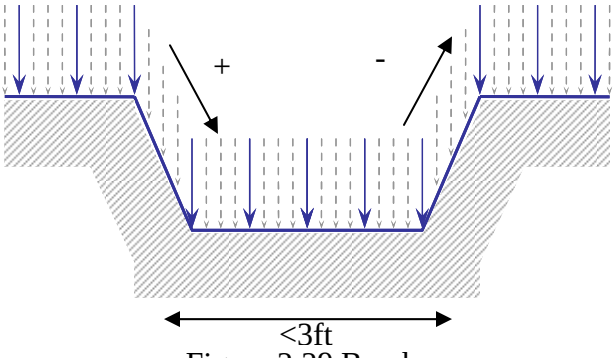

Figure 2.29 Breaks

2.4.3 Slab Curling

Curling is the distortion of a slab into a curved shape by upward or downward bending of the edges. This distortion can lift the edges of the slab from the base leaving an unsupported edge or corner which can crack when heavy loads are applied. Sometimes, curling is evident at any early age. In other cases, slabs may curl over an extended period of time.

2.4.3.1 Methods for Identifying Slab Curling

Several methods were studied to extract the curling of the slabs from the dummy profile. The methods studied were; (1) Gaussian Band-Pass Filter (GBPF) method, (2) Joint Time Frequency (JTF) analysis, (3) wavelet analysis method, and (4) Discrete Slope Method. The moving average of the profiles is not critical for identifying curling because the moving average filters are low-pass filters and do not eliminate the curling after passing the profile into the filters.

The Gaussian Band-Pass Filter extracts certain frequency contents from the Fast Fourier Transform (FFT) algorithm. Thus, the curling can be extracted after performing FFT to the profile and then applying the filter to the transformed profile. Figure 2.31 shows the artificial curling used in the dummy profile along with the curling that was extracted using the GBPF method. The curling was extracted with a phase lag.

Figure 2.32 shows the curling profiles extracted from the dummy profile, using three different wavelet analyses; db10, sym8, and coif5 wavelets.

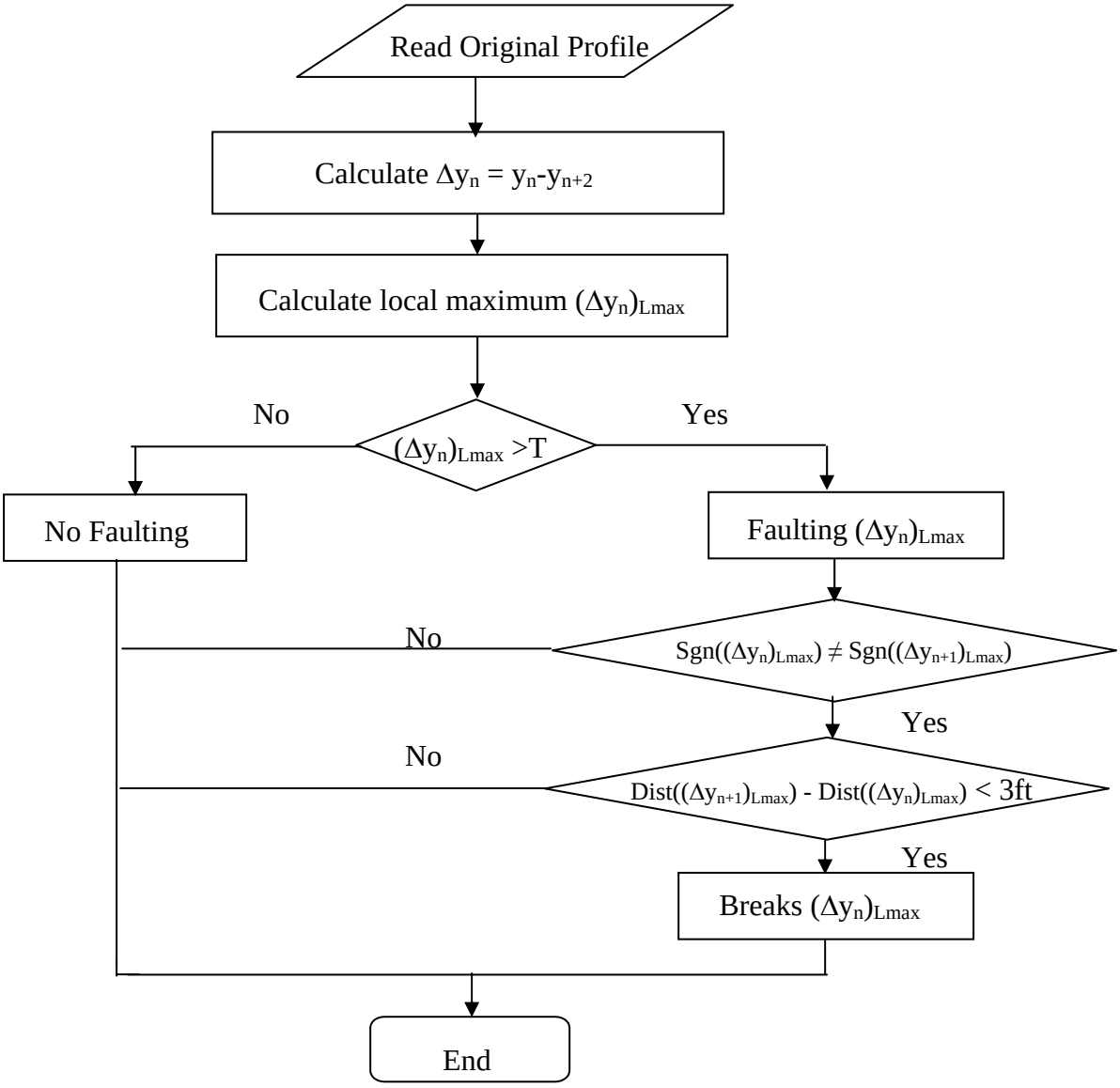

Figure 2.30 Breaks detection algorithm

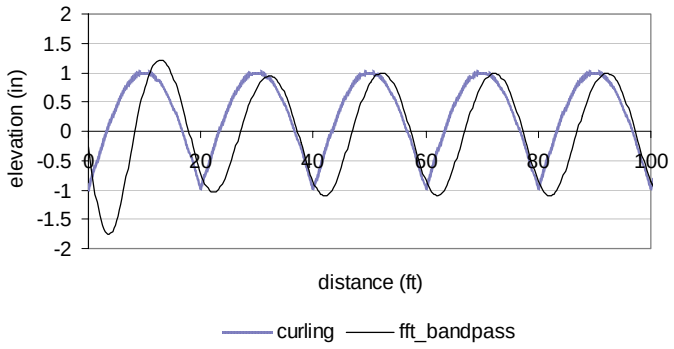

Figure 2.31 Created curling and extracted curling

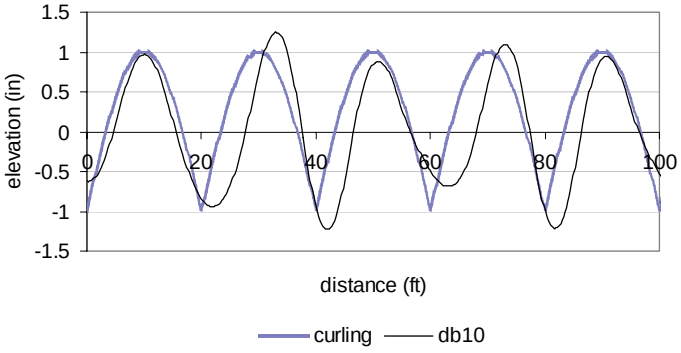

(a) Extracted curling of the dummy profile using db10 wavelets

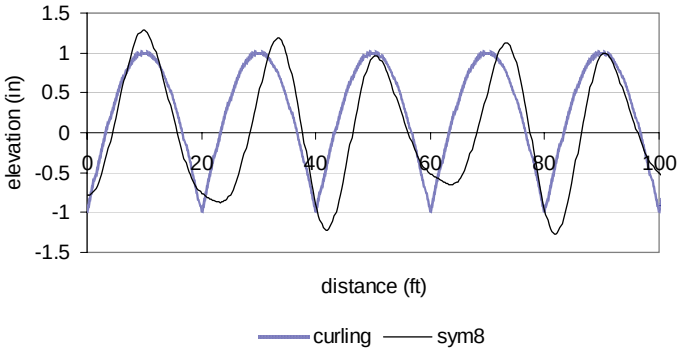

(b) Extracted curling of the dummy profile using sym8 wavelets

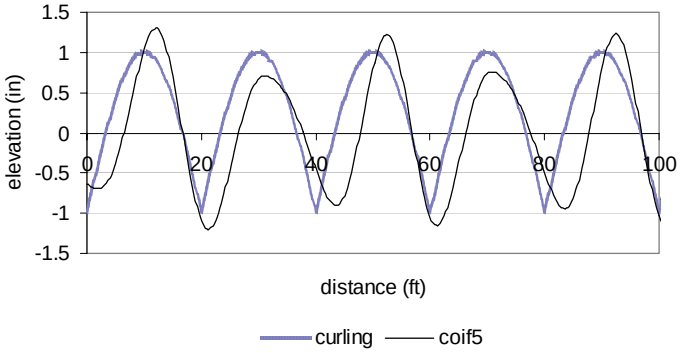

(c) Extracted curling of the dummy profile using coif5 wavelets

Figure 2.32 Created curling and extracted curling

Joint time frequency analysis was performed on the dummy profile and the LTPP profile (section 19-0217). The joint time frequency analysis calculates the frequency energy distribution along with the time/distance. Thus, it overcomes the weakness of the Fourier Transform which only provides the overall frequency content but time information.

Although, the joint time frequency analysis method is powerful for electrical and mechanical signals, it was not efficient for the analysis of pavement profiles. Figures 2.33 through 2.35 show the Wigner-Ville Distribution (WVD), Pseudo WVD (PWVD), and

Smoothed Pseudo WVD (SPWVD) of the dummy profile. As it can be seen from the Fourier spectrum –placed at the left hand side of the time frequency distribution- the major energy is concentrated in relatively low frequency components.

The Discrete Slope (DS) method is used to detect discontinuities in digital image processing. It is similar to the DED method in the sense that it takes the difference of the elevation heights. But the difference is that the slope (difference in elevation) is taken from the adjacent sample points. Figure 2.36 shows a simulated profile and the corresponding slope.

It can be seen from figures 2.31 through 2.35 that the GBPF method seems to work better than wavelet and time-frequency methods. However, this method produces a phase lag or time shift which could affect the localization. The DS method produces same order of error in magnitude but more accurate in localization.

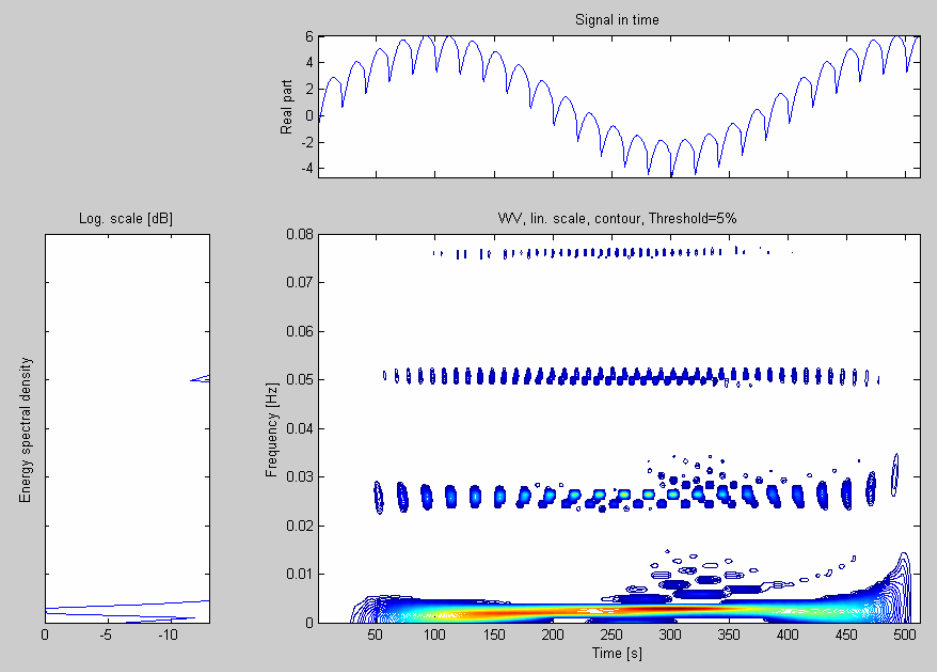

Figure 2.33 Wigner-Ville joint time frequency distribution of the dummy profile

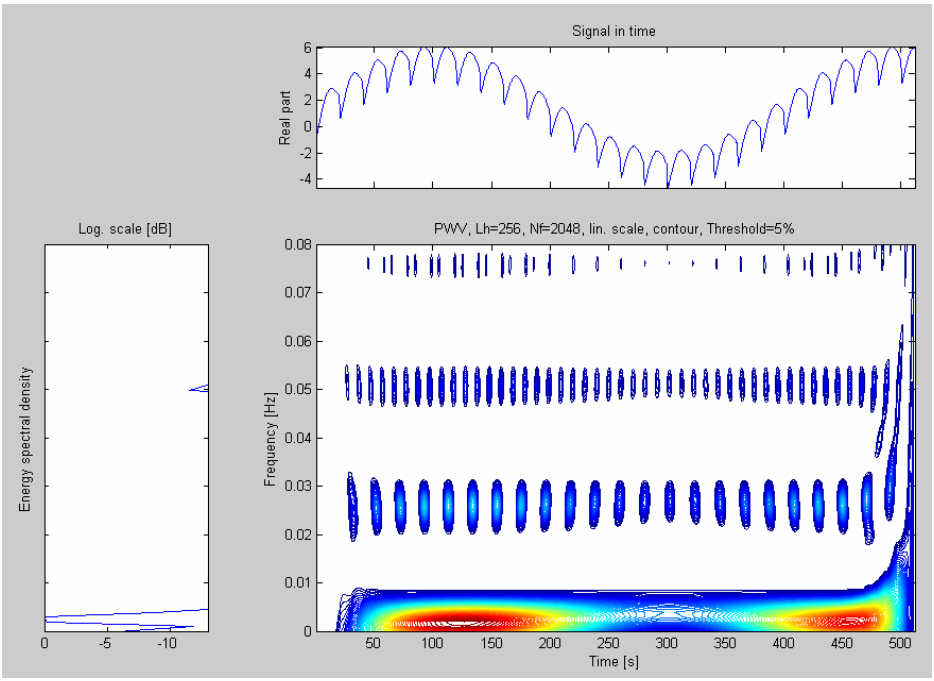

Figure 2.34 Pseudo Wigner-Ville joint time frequency distribution of the dummy profile

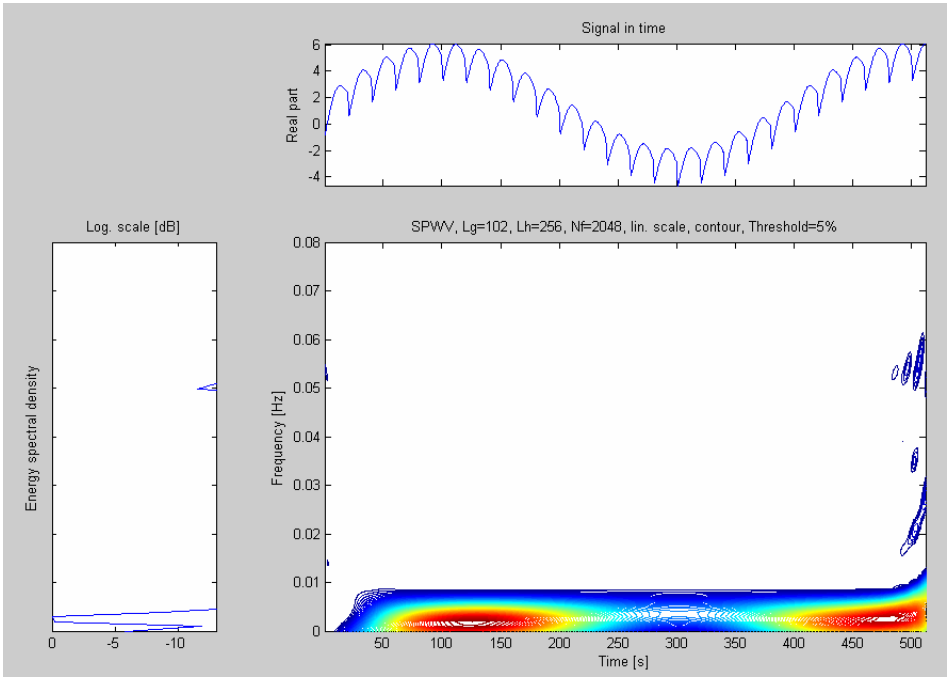

Figure 2.35 Smoothed Pseudo Wigner-Ville joint time frequency distribution of the dummy profile

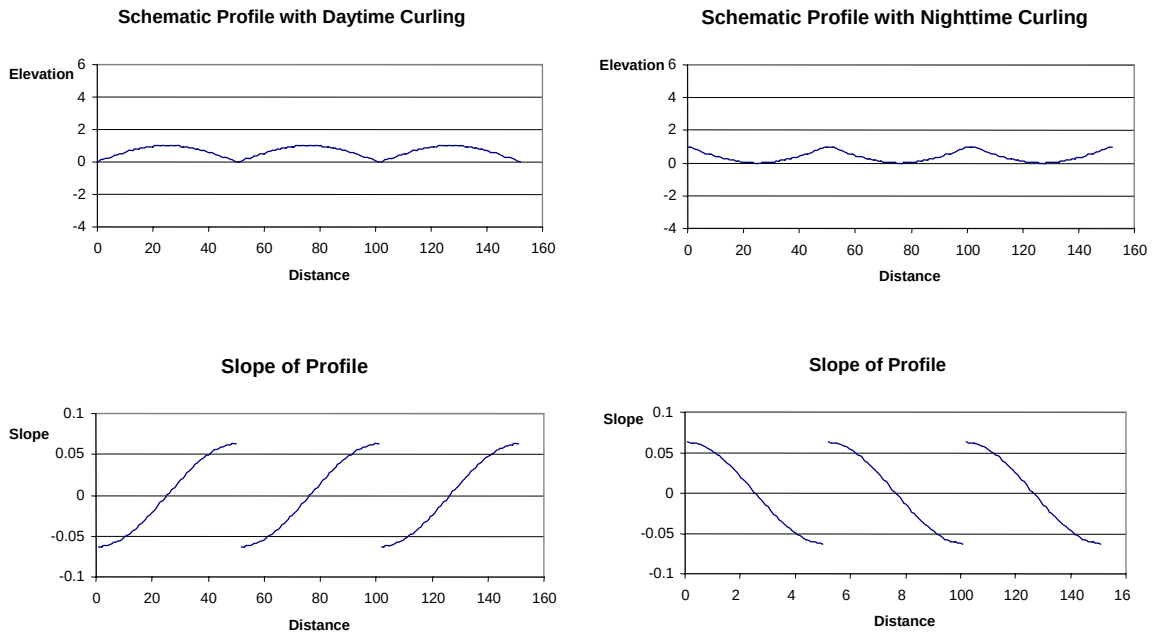

Figure 2.36 Created curling and extracted curling with DS

2.4.3.2 Discrete Slope Method

Since we are looking for discontinuities in the slope of the profile, the discrete slope (DS) method was identified as a method to detect slab curling. This method has been used in signal and image processing for its capability to detect discontinuities. It is similar to the DED method in the sense that it takes the difference in elevation. But the difference is that the slope (difference in elevation divided by the distance between the points) is taken from the adjacent sample points. It is noted that the topography has an impact on the curling magnitude detection. To filter out the topography, a high-pass filter (300 ft long cut-off wavelength) was applied. Then, to eliminate the effect of profile roughness and micro-curling, a low-pass filter (5 ft short cut-off wavelength) was applied. Figure 2.37 shows the results after each step.

A number of approaches have been used for removing the long-wave topography from the measured profile (e.g. moving average, 2-pole Butterworth, 4-pole Butterworth (Sayers et al., 1996), etc.). The principles of several filtering techniques have been discussed in the pavement smoothness literature (Chang et al., 2005). In this analysis, we have used the Butterworth filters before implementing the specific roughness detection algorithms. These filters are superior since they have the following characteristics (Orfanidis, 1996):

- Smooth response at all frequencies
- Monotonic decrease from the specified cut-off frequencies

- Maximal flatness, with the ideal response of unity in the passband and zero otherwise.
- Half-power frequency that corresponds to the specified cut-off frequencies

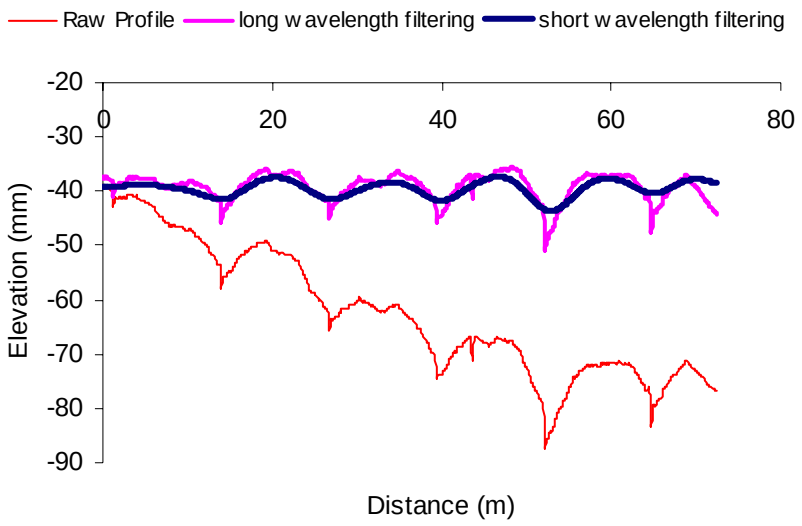

Figure 2.37 Original and filtered profiles

Since a 2-pole Butterworth filter add a phase lag to the filtered profile, a 4-pole Butterworth was needed. Finally, to compute curling, differences in elevation between the point that corresponds to the local maximum of the slope function and the next point where the slope function is zero is computed (Figure 2.38). The algorithm for the curling detection is described in Figure 2.39.

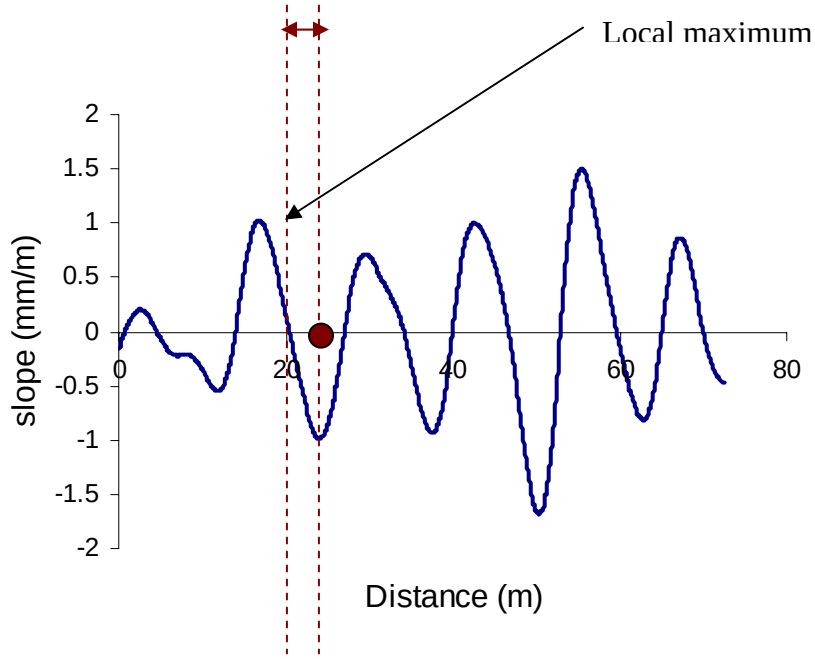

Figure 2.38 Detection of local maxima of the slope function

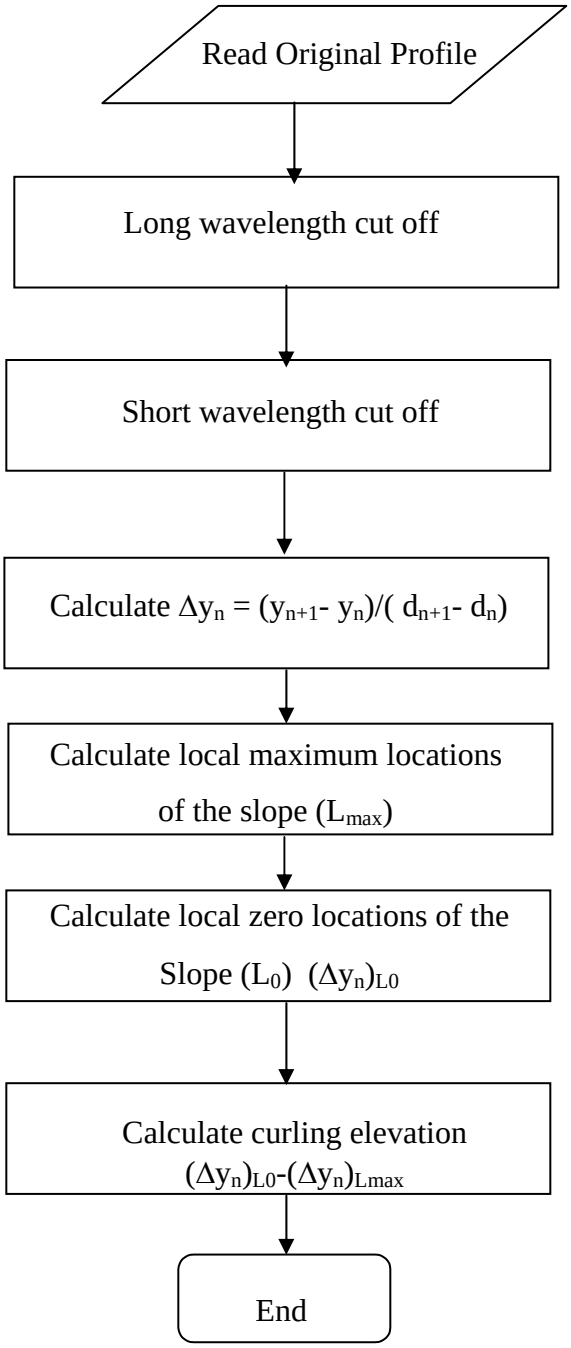

Figure 2.39 Curling detection algorithm

2.5 FIELD TRIALS

Different methods were used in the study, including wavelets, time-frequency and discrete methods. The discrete elevation difference method (DED) was selected for faulting and breaks detection, and the discrete slope method (DS) was selected for curling detection. In order to evaluate and verify the detection tool, it is necessary for the research team to conduct a field survey. First, the research team decided on the criteria for selecting the pavement sections. These criteria are summarized in Tables 2.1 and 2.2.

Table 2.1 shows the minimum number of pavement sections that needs to be visited with each distress type and severity level. However, this table assumes that in a pavement section, there is only a single type of distress corresponding to a single severity level. Thus, it should be noted that the number of pavement sections to be visited can be reduced significantly if a pavement section has a large number of distresses at different severity levels, which was the case.

Table 2.2 shows the definition of the severity levels of different distresses. Since there is a similar trend in the profile data for faults, breaks, bumps, and depression, the definition of severity levels for these distresses may be combined. The severity definition of the above distresses is the same as those used by Pathway's fault detection algorithm which again agrees with MDOT's definition of severity level for faults.

Table 2.1 Number of Pavement Sections[1] for Verification of Roughness Diagnosis Tool

Pavement Type		Rigid	
Distress Type		Faults/Breaks	Curling
Severity Level[2]	Low	3	3
	Medium	3	3
	High	3	3

Notes: [1] A pavement section is 0.1 mile long. [2] A given section may have all three severity levels.

Table 2.2 Definition of Severity Level

	Severity Level		
Distress Type	Low	Medium	High
Faults, Breaks, Bumps and Depression	$\leq$ 0.25 inch	$\geq$ 0.25 inch, $\leq$ 0.75 inch	$\geq$ 0.75 inch
Curling	N/A	N/A	N/A

2.5.1 Field Trips

The first visit to the field was held on Tuesday, July 26th, 2005. The trip was scheduled for measuring faults in rigid pavements. An interstate highway was selected in the University region. Section 1 was located on I69 close to exit 84 (Airport road). The

pavement type is rigid with a joint spacing of 41 feet. The selected pavement section was approximately 0.4 miles long and has a lot of faulting at the joints and cracks. The measurements were taken in between stations 386+36 and 408+95 using the digital faultmeter (also called the Georgia faultmeter) at the left and right wheel paths and at the center of the lane. The right wheelpath was 3 ft away from the shoulder and the left wheelpath was 5.75 ft apart from the right wheelpath. These represent rough locations of where Pathway lasers would fall. Table 2.3 summarizes the number of measured faults in terms of the severity level defined in Table 2.2.

The second visit was held on Thursday, October 27th, 2005. Section 2 was located on I-69 just before exit 105 (Perry Exit). Section 3 is about a mile down the road from the end of the first one. Section 2 was approximately 0.52 mile (2725 ft) long and has a lot of faulting at cracks. The measurements were taken between stations 693+00 and 720+00. Section 3 was approximately 0.52 mile (2724 ft) long. The measurements were taken between stations 773+00 and 800+00. Both sections are rigid pavements with a joint spacing of 41 feet.

The third visit was held on Tuesday, November 8th, 2005. Section 4 was located on I-69 east bound at mile marker 130. It is also a rigid pavement with a joint spacing of 41 feet. The selected pavement section was approximately 0.86 miles (4525 ft) long. The measurements were taken between stations 130+00 and 174+00.

In sections 2 through 4, faults were measured at the left and right wheel paths using the Georgia Faultmeter.

Appendix A summarizes the measured faults at each section. Table 2.4 summarizes the number of measured faults in terms of the severity level and the extreme magnitudes of faults in each of section 2 through 4.

Table 2.3 Summary of measured faults in I69

	Counts			
Severity level	Low	Medium	High	Total
Individual measurements	199	16	1	216
Average fault along transverse direction	69	3	0	72

Table 2.4 Summary of measured faults in each section

Severity level	Section 2				Section 3				Section 4			
	Low	Medium	High	Total	Low	Medium	High	Total	Low	Medium	High	Total
Individual measurements	124	4	0	128	57	12	0	69	150	48	0	198
highest magnitude (in.)	0.555				0.378				0.5438			
lowest magnitude (in.)	-0.114				-0.1498				-0.4258			

The research team had also taken repeated measurements in order to evaluate the accuracy of the measurement device. Appendix B summarizes these measurements.

In order to verify the methods using the collected data, the profile data for the same pavement section were requested to be used in the developed algorithms.

2.5.2 Results

Figures 2.40 through 2.42 show the correlation of the predicted magnitude and location with measurements for each site. As can be seen from these figures, the predicted magnitude and location for each site are linearly dependent on the measured results. Statistical analyses were performed to study the accuracy of the method. Using the "linear regression through the origin method" with 95% confidence interval, a very good fit was obtained, as can be seen in all these figures. However, each figure shows a bias, although it is very small; this error could be the result of error in fault measurements or inaccuracy of profile data. Comparing the slopes from successive figures, it can be seen that the bias in the measurements was slightly reduced after each field test (slope value closer to unity). We conclude that the DED method was able to detect and compute the fault magnitude with a reasonable accuracy.

Three breaks were reported during the field test in Site 1. The tool was able to detect all three breaks with a comparable magnitude and location. Site 1 also had severe early morning (upward) curling (Figure 2.43). The tool was also able to detect the curling magnitude and frequency (Figure 2.44).

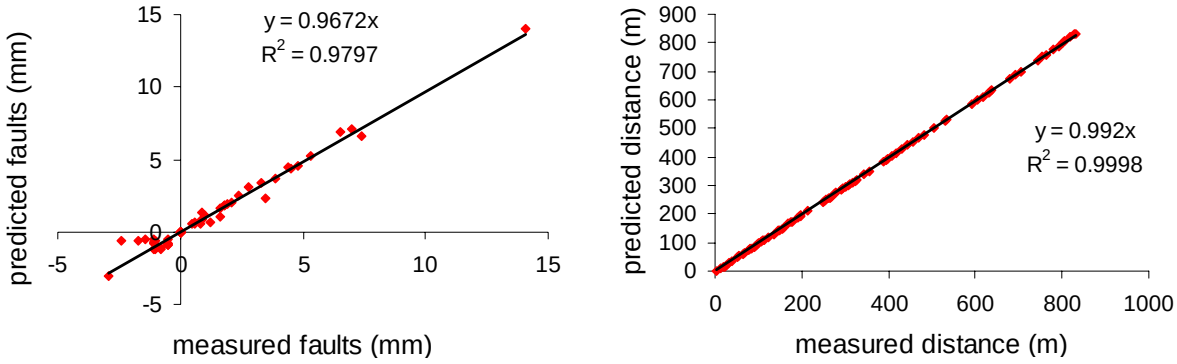

(a) (b)

Figure 2.40 Correlation analyses for Site 2 (a) magnitude (b) location

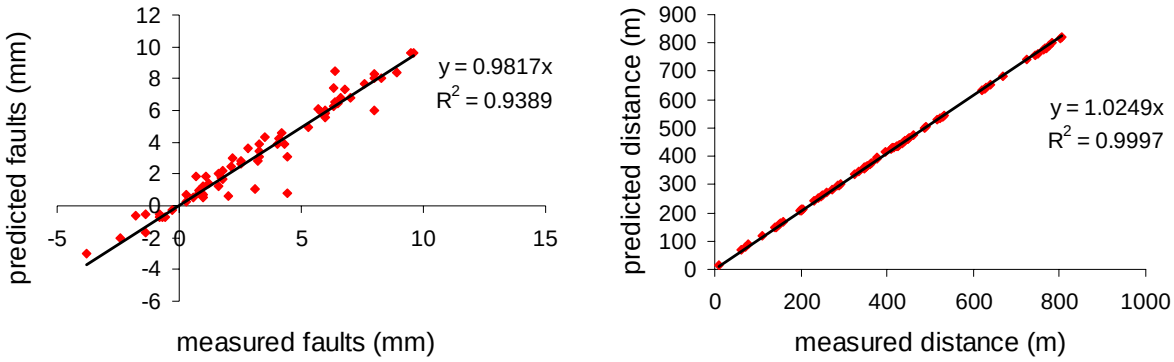

(a) (b)

Figure 2.41 Correlation analyses for Site 3 (a) magnitude (b) location

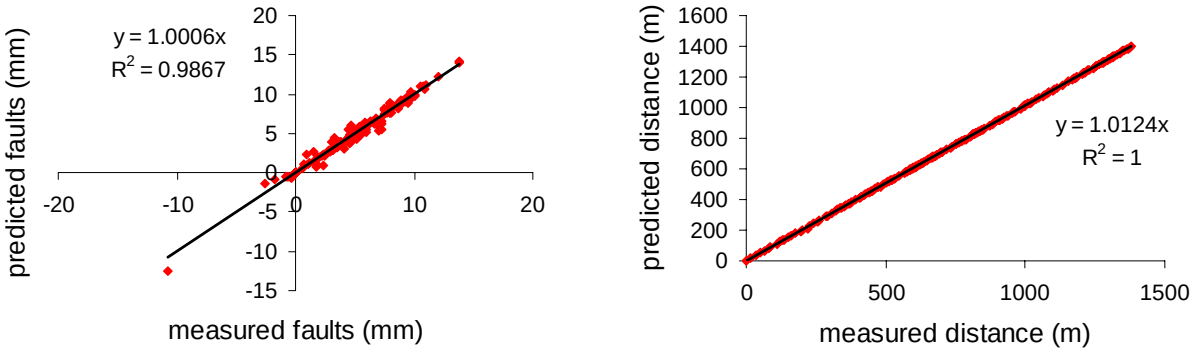

(a) (b)

Figure 2.42 Correlation analyses for Site 4 (a) magnitude (b) location

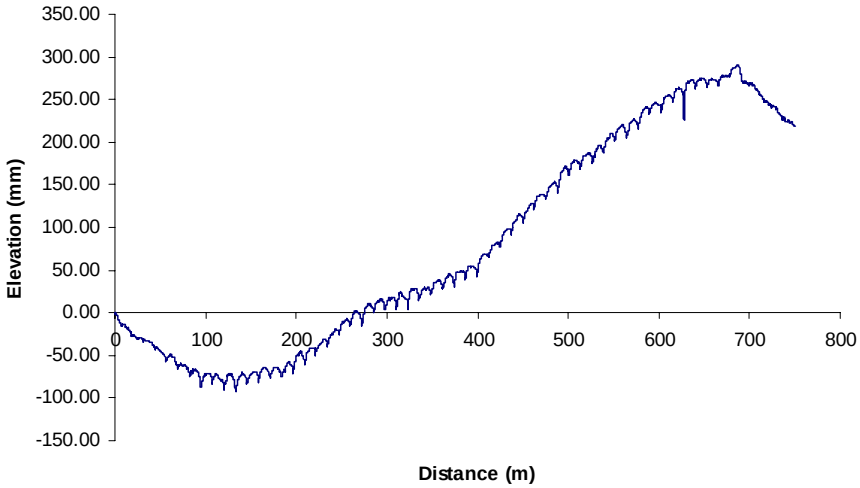

Figure 2.43 Raw profile with severe curling (Site 1)

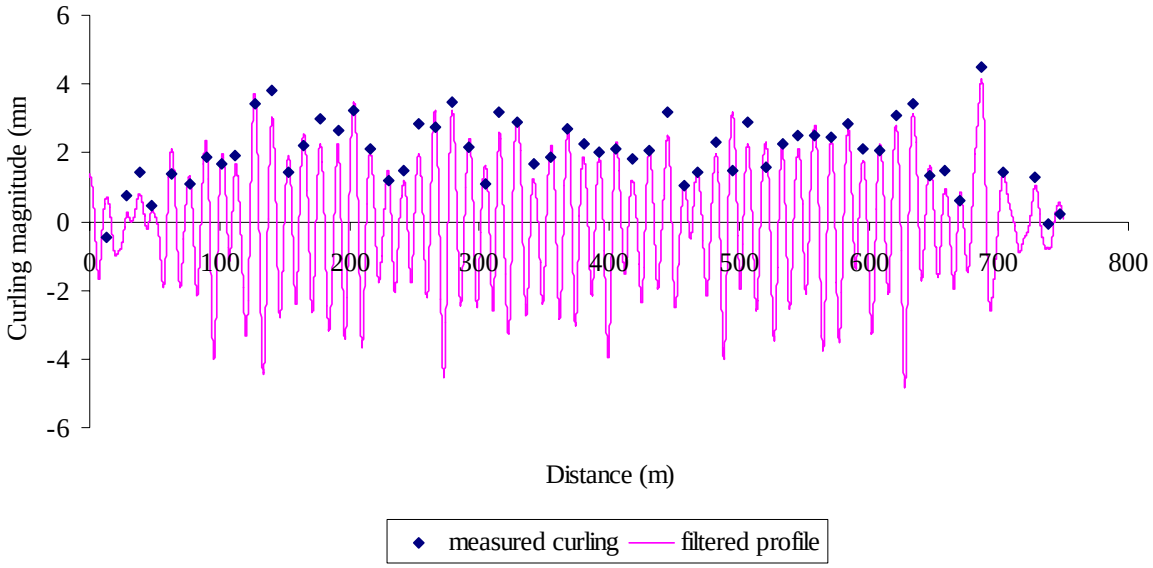

Figure 2.44 Filtered profile and curling magnitude

CHAPTER 3
DEVELOPMENT OF A PROFILE-BASED DIAGNOSTIC TOOL FOR IDENTIFYING SURFACE DISTRESSES

3.1 INTRODUCTION

Chapter 2 was intended to choose and finalize the most accurate and reasonable identification method for surface distresses. Various profiles were studied with several signal processing techniques. The Pathway method was also reviewed. Based on the preliminary findings, user-friendly software was developed. The distress detection tool is an engineering software application that allows users to view and analyze longitudinal pavement profiles.

3.2 USER MANUAL FOR DISTRESS DETECTION TOOL

The software is an excel file with macros. Macros are written in VBA language. To make sure that the software is running, the security level for Excel must be set to "***Medium***" or "***Low***". Figure 3.1 shows how to change the security level. When you run the application, a security alert message will be displayed (Figure 3.2). Then, you should accept and click on "***YES***". The main window appears giving the opportunity to the user to run or close the application (see Figure 3.3).

The roughness localization window (Figure 3.4) contains three tabs each of them corresponds to one distress type: Faulting, Breaks and Curling. Also, the window allows the user to import a raw profile (*.ERD file) and then choose left or right wheelpaths. If ERD files are not available or MDOT changes contractors, the user could create his/her own ERD file by following the instructions in section 3.2.1.1.

3.2.1 Import/Export Windows

The application allows the user to import ERD files including the general information and raw profile, and export results in an excel file format. An ERD file contains two independent sections, the header and data. The header part contains only text, and the data part contains only numbers. The numbers are written in text form (Sayers, 1987).

3.2.1.1 ERD files

3.2.1.1.1 The Header

The ERD file header consists of a series of conventional readable text lines. These lines contain the information used by post-processing tools to read the numerical data. As a minimum, the header contains three lines of text:

- The first line identifies the file as following the ERD format.
- The second line describes the way that the numerical data are stored in the data section of the file.
- The third required line is an END statement that indicates the end of the header portion. Any number of optional lines can be included between line #2 and the END line.

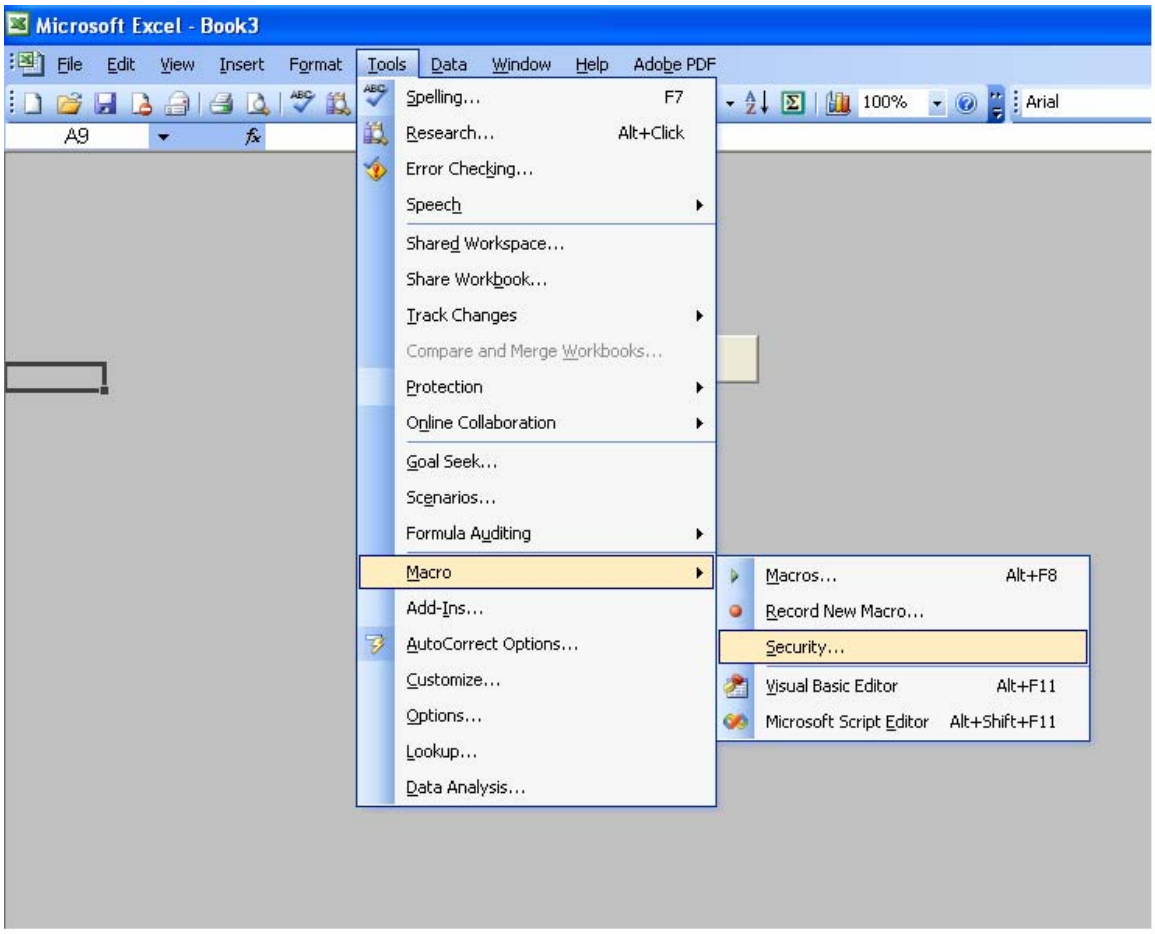

Figure 3.1 Set up of the security level

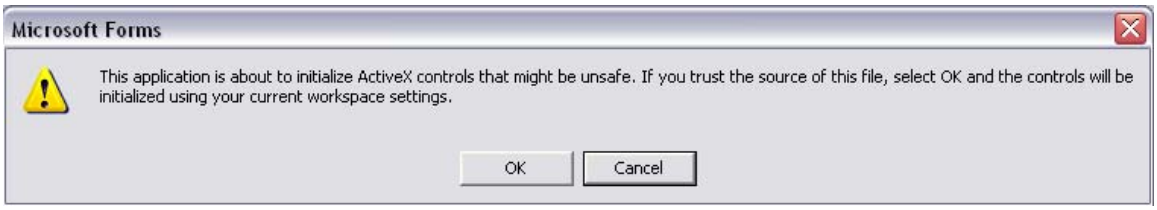

Figure 3.2 Security alert message

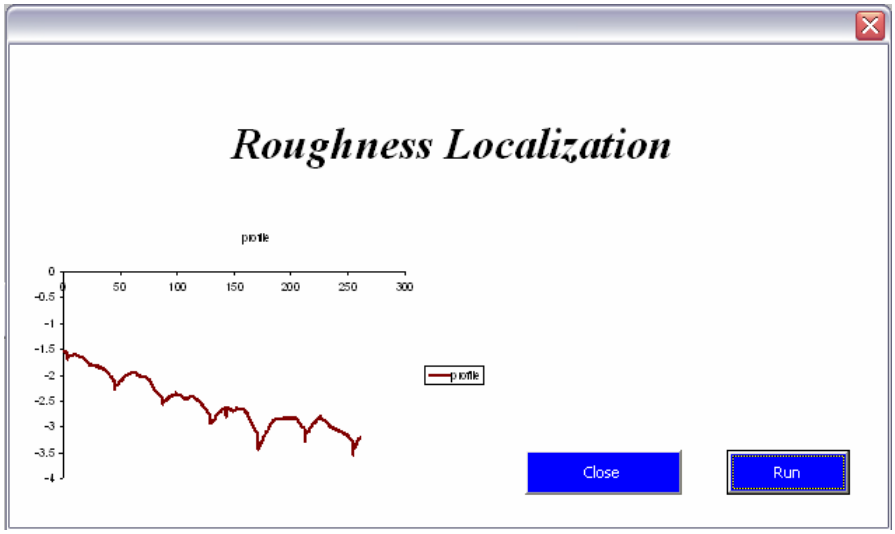

Figure 3.3 Main window

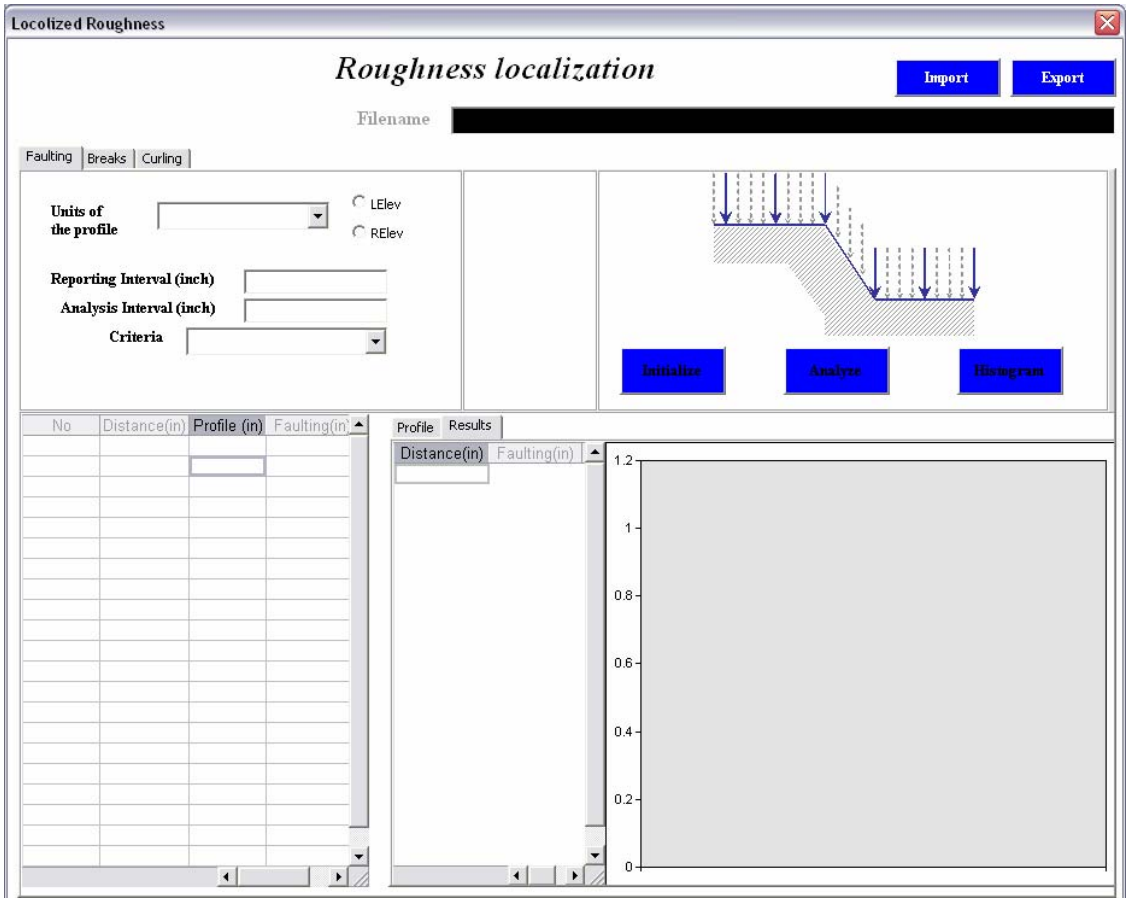

Figure 3.4 Localized roughness window

Table 3.1 summarizes the lines in an ERD file, and describes the parameters used in line #2 to describe the numerical data.

Table 3.1 Summary of records in an ERD file header

Line No.	Description
1	`ERDFILEV2.00` -- identifies file as having ERD format
2	NCHAN, NSAMP, NRECS, NBYTES, KEYNUM, STEP, KEYOPT -- use commas to separate numbers: • NCHAN [integer] = Number of data channels. • NSAMP [integer] = Number of samples for each channel. • NRECS [integer] = Number of records of data. • NBYTES [integer] =Number of samples per record. • KEYNUM[integer] Indicates how the data are stored. o 5, 15 = Formatted floating-point (text). The format must be specified using the FORMAT keyword. For KEYNUM=5, the data are stored with all channels for the first sample together, then all channels for the second sample, etc. For KEYNUM=10,11, and 15, the data are stored with all samples for the first channel together, then all samples for the second channel, etc. • Step [real] = sample interval (e.g., time step) • KeyOpt [integer] = auxiliary number used by some programs
	Optional records. Each record begins with an 8-character keyword, followed by information associated with that keyword.
Last Line	`END` -- indicates the end of the header

Figure 3.5 shows an example header which is fairly brief, consisting of the three required lines and four optional lines. (The optional lines are the ones beginning with the keywords TITLE, SHORTNAM, XLABEL, and XUNITS.)

Looking at the second line of the file shown in Figure 3.5, we see that the file contains data for 2 channels, with 529 samples per channel, stored as 1 record, that the data storage format is type 5, that the interval between samples is 1.00, and that the status of the auxiliary numbers is -1. The header shown in Figure 3.5 includes names of the units for each channel, as identified with the keyword UNITSNAM. The name of units for the first channel, ft, has only two characters. Thus, it is followed by six spaces so that the name for the second channel, ft, begins in the correct column position.

Using the format of the ERD files that MDOT gave to the research team, the input files (*.ERD) should include all the lines in the heading presented in figure 3.6. The software will work properly only if the input files follow the mentioned format.

```
ERDFILEV2.00
      2,    529,     -1,      -1,      5,  1.00000    ,     -1,
TITLE   1993 RPUG Study, Dipstick, Section 1, Measurement 1
SHORTNAMLElev.  RElev.
UNITSNAMft      ft
XLABEL  Distance
XUNITS  ft
END
  0.000000      0.000000
  0.416667E-03 -0.141667E-02
  0.416667E-03  0.583333E-03
  0.666667E-03  0.916667E-03
  0.133333E-02  0.133333E-02
  0.750000E-03 -0.166667E-02
 -0.300000E-02 -0.458333E-02
 -0.558333E-02 -0.500000E-02
 -0.625000E-02 -0.658333E-02
 -0.775000E-02 -0.825000E-02
Etc.
```

Figure 3.5 Short Header for an ERD File with Text Data.

```
ERDFILEV2.00
      2,   9840,     -1,      1,      5,      0.2459307,     -1,
TITLE   I69
SHORTNAMLElev.  RElev.
UNITSNAMft      ft
XLABEL  Distance
XUNITS  ft
SURVDATE 05/07/2005 12:11
DISTRICT 6
COUNTY   0
ROADFROM JCT CONN-96
ROADTO   JCT US-127
ROADFRMP 4.510
ROADTOMP 4.968
IRILWP   0
IRIRWP   0
DATAFR   1
END
```

Figure 3.6 Example of required headings for the input files

3.2.1.1.2 Data

The data part of the ERD file contains nothing but numbers, organized into columns and rows. The form in which the numbers are stored depends on the value of the KEYNUM parameter from line 2 of the header (see Table 3.1). The total number of

values that will appear in the data section is NCHAN x NSAMP. All of the numbers in the data portion are stored in the same format, and there can be no missing values.

3.2.1.2 Import window

The "***Import***" button in the localized roughness window opens a new screen asking the user to choose an ERD file name. Then, users should click on the "***Open***" button such that the application will extract all the relevant information about the site (Figure 3.7).

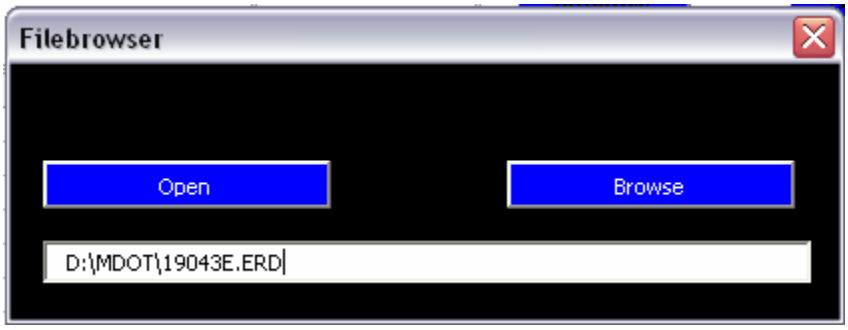

Figure 3.7 Import file window

3.2.1.3 Export window

The "Export" button in the localized roughness window opens a new screen asking the user to choose a file name and its path. Then, users could export to excel results using the "***Save***" button. Users should enter a file name followed by the extension ".xls" to export to excel file (Figure 3.8).

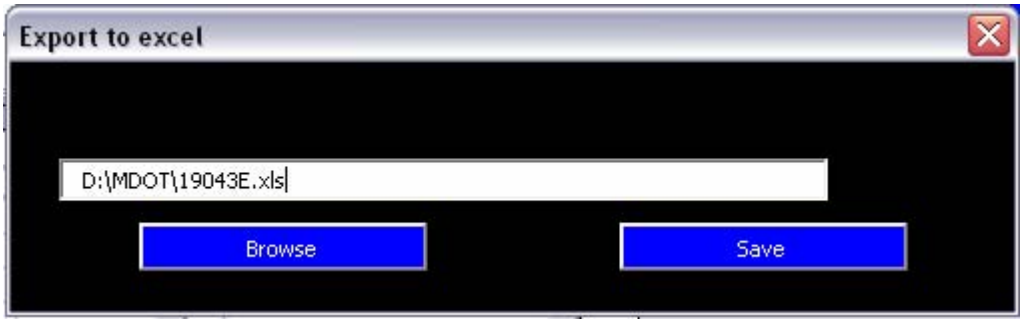

Figure 3.8 Export results window

3.2.2 Faulting Detection Window

Figure 3.9 shows the fault detection window. Users should choose between the right and left wheelpath from the raw profile. To do that, they should check the radio point that corresponds to the preferred wheelpath. Once checked, the application copies the raw profile to the column "***Profile***".

Before analysis, users should specify the threshold (in inches) as well as the reporting interval. If the worksheet is not empty, users should click on the "***initialize***" button. Then, they should click on the "***analyze***" button.

The output for the analysis will be shown on the "***results***" tab (Figure 3.9). The application allows users to plot the raw profile on the "***profile***" tab (Figure 3.10).

In order to get summary statistics as well as faulting distribution according to their severity, the user should click on the "***histogram***" button (Figure 3.11). Users should enter a bin range to get fault distribution; otherwise, default values are used (corresponding to the severity level selected by the research team and defined in Table 2.1); i.e.,

- 0.25 low severity level
- 0.5 Medium severity level
- 0.75 high severity level

Figure 3.9 Fault detection results window

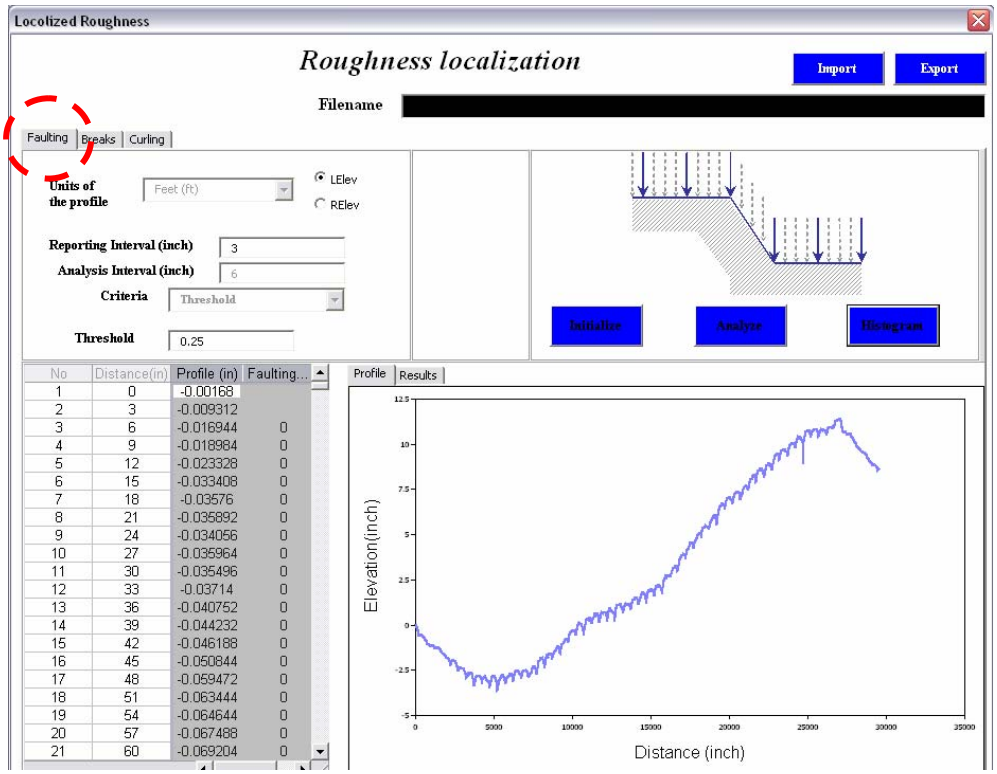

Figure 3.10 faulting detection window displaying the original profile

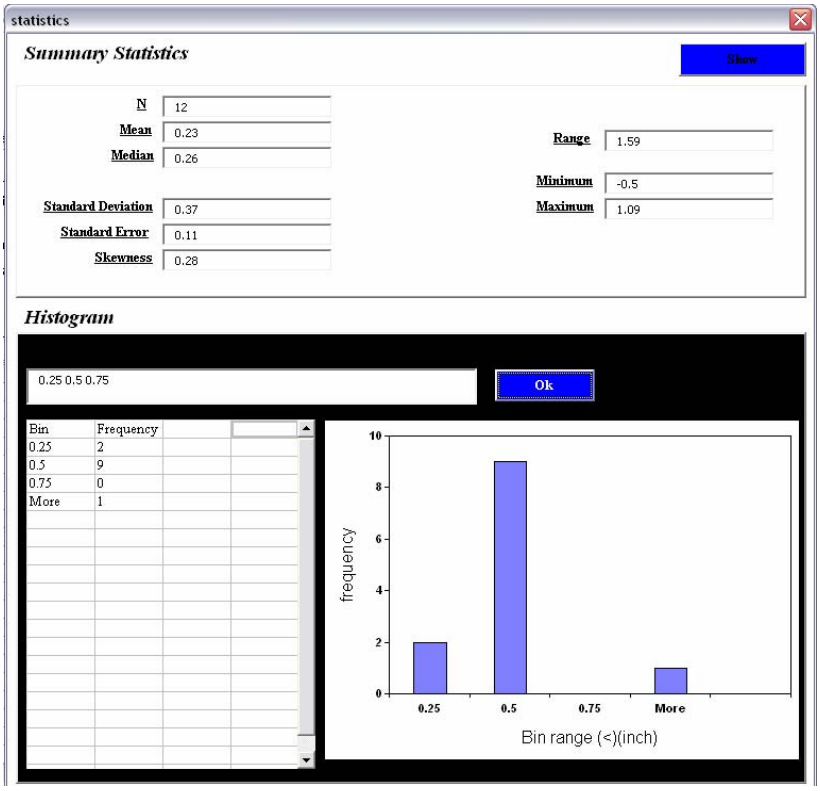

Figure 3.11 Fault results summary and distribution window

3.2.3 Breaks Detection Window

Figure 3.12 shows the Breaks Detection window. Before detecting breaks, first, the module detects any difference in elevation. Since, this part is the same as the fault detection module, users should specify the same inputs as for detecting faulting; i.e reporting interval and threshold. Second, if the sign of two successive faults is different, the Breaks detection module checks the distance between them: if the distance is less than 3 feet, it is considered break; otherwise, there is no break. The 3 feet threshold can be changed; however, the program would have to be modified to do that. This module gives as a result:

- Starting Point of the break;
- Width of the break; (length along the profile)
- Fault magnitude at the stating point; and,
- Fault magnitude at the end point

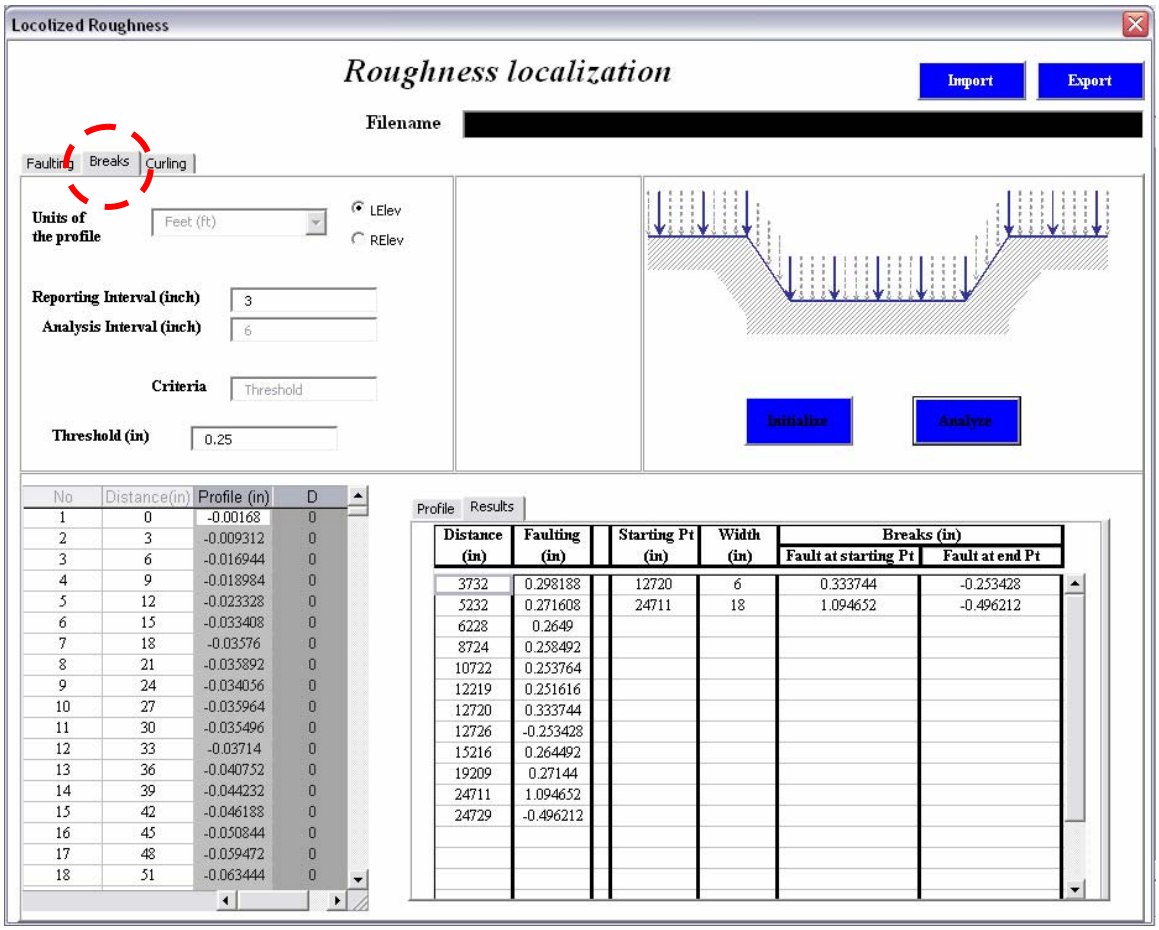

Figure 3.12 Breaks detection results window

3.2.4 Curling Detection Window

Figure 3.13 shows the Curling Detection Module. First, the module cuts off the long wavelengths (high frequency) and the short wavelengths (low frequency) to filter out the topography. A 4th order Butterworth band-pass filter is used. Second, the module displays the original and the filtered profile as shown in Figure 3.14. Third, the slope of the filtered profile will be computed and the local maximum and zero points of the slope function will be detected. At the end, the zero point's location and the difference in elevation between zero and maximum point will be resumed. Users should specify only the reporting interval. Note that changing the reporting interval would not affect the results.

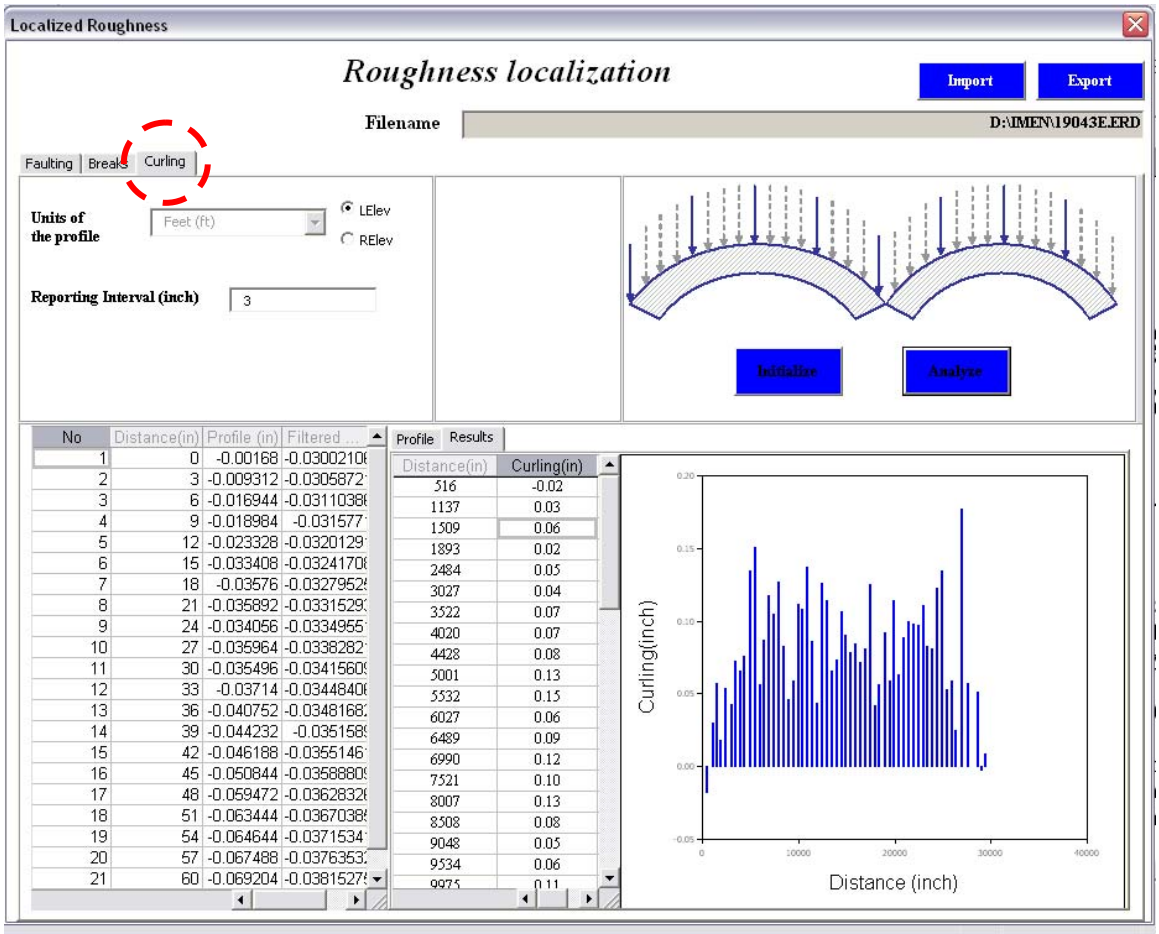

Figure 3.13 curling detection results window

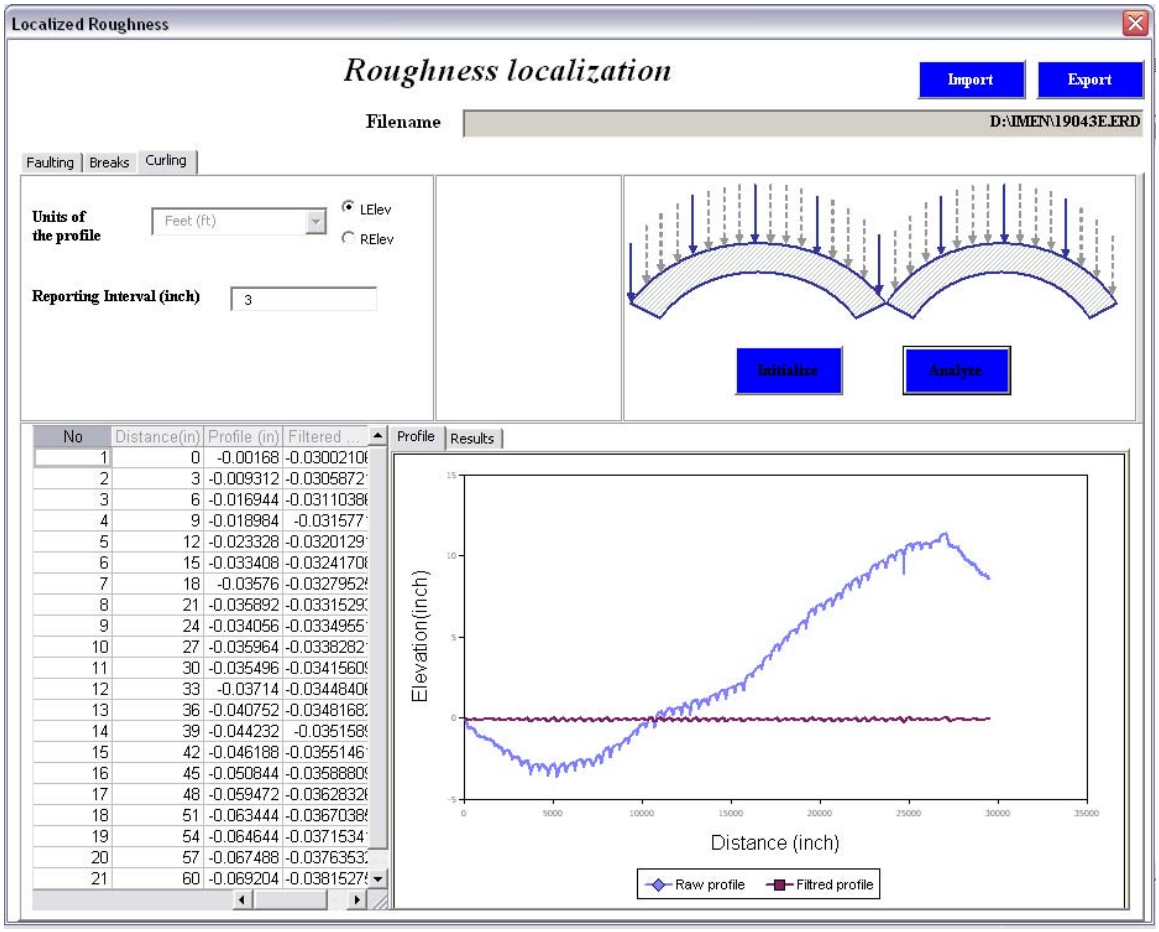

Figure 3. 14 curling detection window displaying the original and the filtered profile

CONCLUSION

The aim of this study was to develop a tool for detecting surface distresses that are not identifiable from the video imaging using the longitudinal profiles of a pavement surface. As stated previously, the candidate distresses can be summarized into two categories:

- Distresses that appear as profile discontinuity – faults and breaks
- Distresses that appear repeatedly with some period – curling of PCC pavements

The purpose of the work done in Phase I was to review and identify the most appropriate methods for detecting surface distresses. These methods include: wavelet analysis, joint time-frequency analysis and discrete methods. The methods were evaluated using simulated profiles and profiles of LTPP sections. The study was aimed at selecting and finalizing the most accurate method. The discrete elevation difference method was selected for fault and break detection. The discrete slope method was selected for curling detection. Field trials were held in different sections in Michigan so that the selected methods could be validated and finalized. The newly developed algorithms were able to detect the magnitude of faulting, breaks and curling with an R^2 of 0.97 and standard error (SE) of 0.25 mm. The localization was also highly accurate (R^2 =0.99). These results indicate that the methods developed in this study can capture relevant information about these roughness features with reasonable accuracy.

The final step was to develop a user-friendly, window-based computer software system for detecting and quantifying new distresses (faulting, breaks and curling). The software system includes the following features:

- An input and output system for handling the required data
  - selecting profile data for analysis
  - changing parameters (criteria/decision rules) for distress identification methods
  - storing/reporting the detected surface distresses

- A means to display a combination of profile data and results.

A user manual is included in this report. The data collected from the field trials and used in the evaluation of the selected method are presented in Appendix A. A copy of the software and the raw profiles of the field trial sections are attached to this report.

This new tool could be used as a complementing module for the existing PMS system. It can be used to enhance the PMS database; for example, by adjusting the distress points for faulted cracks..

REFERENCES

Attoh-Okine, N. O. and Mensah, S., Characterizing pavement profile using wavelets analysis. Constructing Smooth hot mex asphalt pavements, ASTM STP 1433, 2003

Byrum, C. A high speed profiler based slab curvature index for jointed concrete pavement curling and warping analysis. Ph.D Dissertation. University of Michigan. 2001

Chang ,G.K., Dick, J.C., and Rasmussen, R.O. (2005), ProVAL 2.7 User's Guide, http://www.roadprofile.com/.

De Pont and J. J. Scott, A, Beyond road roughness – interpreting road profile data., Road & Transport Research, v8, 1999, p12-28

Fernando, E and Bertrand, C., Application of profile data to detect localized roughness., Transportation Research Record, n 1813, 2002, 02-4050, p 55-61

Orfanidis, S.J. (1996), Introduction to signal Processing, Prentice-Hall, Upper Saddle River, New Jersey.

Sayers, M.W. ERD Data-Processing Software Reference Manual. Version 2.00 Univeristy of Michigan Transportation Research Institute Report UMTRI-87-2, (1987) 109 p.

Sayers and Karamihas, Interpretation of Road Roughness, UMTRI 96-19, June 1996.

APPENDIX A: FIELD TRIALS DATA

SITE 1

Distance		Faulting (mm)				Explanation	Other
Feet	Inches	Left	Center	Right	Average		
0	0	1.5	1	1.5	1.33	Station 386+36	
41	2	2.3	2.4	3.1	2.60	Joint	
82	3	0.9	1.9	3.6	2.13	Expansion Joint	
123	4	0.6	1.2	1.6	1.13	Joint	
164	2	0.5	1.4	1.7	1.20	Joint	
191	7	Pothole with D = 6 in.					
178	3	Pothole with D = 6 in.					
205	6	1.1	2	2	1.70	Joint	
246	9	0.2	1.2	1.7	1.03	Joint	
271	8	Pothole with D = 4 to 8 in.					
287	11	2.3	4	5.5	3.93	Joint	
301	4	6 in. break (3ft)		2 in. wide		Crack	
331	0	7	6.7	4.5	6.07	Joint	
371	10	2.4	3.9	4.5	3.60	Joint	Negative patch 1ft before joint
413	7	5.3	5.3	4.9	5.17	Expansion Joint	
419	11	1.6	2.3	2.9	2.27	Crack	
435	5			Patch			
454	7	6.5	5.9	5.7	6.03	Joint	
495	8	5	5.7	4.9	5.20	Joint	Shallow pothole (4 to 5 in. wide) at 1 to 2 in. away from left wheelpath
536	8	5.3	5.4	3.9	4.87	Joint	
567	6					Station 392+00	
577	9	3.8	4.5	2.9	3.73	Joint	
607	10	-0.4	0	-2.3	-0.90	Patch start	
614	1	-0.7	-0.3	0.1	-0.30	Patch end	
618	9	0.7	-1	-3.2	-1.17	Joint	
624	9	-0.7	0.5	-0.3	-0.17	Patch start	
630	8	2.4	2.8	1.6	2.27	Patch end	
659	6	6.2	5.2	5.5	5.63	Joint	
667	1					Station 393+00	
700	6	6.3	5.7	5.3	5.77	Joint	

741	7	1.7	2.3	3	2.33	Expansion Joint	
782	6	4.4	4.9	4.7	4.67	Joint	
823	6	3.8	3.3	3.6	3.57	Joint	
841	1	Pothole					Figure A.1
848	3	-0.8	0.1	0.2	-0.17	Sealed Crack	
864	7	3.5	1.7	1.9	2.37	Joint	
883	11	Pothole					Figure A.2
905	8	5.4	6.3	6.8	6.17	Joint	
946	8	5.4	5.8	4.9	5.37	Joint	
987	7	5.3	6.6	6.7	6.20	Joint	
1028	8	6	1.8	2.9	3.57	Joint	
1069	8	5.1	4.3	5.3	4.90	Expansion Joint	
1092	9	-0.4	0.5	0.3	0.13	Sealed Crack	
1110	7	0.7	0.8	0.4	0.63	Joint	
1132	7	2.1	-0.1	-0.7	0.43	Sealed Crack	Y crack with below (Figure A.3)
1133	11	0	1.8	1.5	1.10	Sealed Crack	
1151	9	3.8	3.4	2.9	3.37	Joint	
1192	9	3.1	5.3	5.9	4.77	Joint	
1233	10	3.3	3.2	2.8	3.10	Joint	
1275	0	6.5	5.8	3.7	5.33	Joint	
1296	11	0.1	0.2	-0.4	-0.03	Sealed Crack	
1316	0	6.4	7.5	7.4	7.10	Joint	
1357	0	1.6	2.9	2.5	2.33	Joint	
1398	1	4.5	5.2	7.2	5.63	Sealed Crack	
1438	0	5.4	5.6	5.7	5.57	Joint	
1453	0	0.5	2.9	3.1	2.17	Sealed Crack	4 in. by 1 ft. of spalling on right wheelpath
1479	11	5.1	5.6	5.5	5.40	Joint	
1520	0	3.8	5	5.2	4.67	Joint	
1562	0	0.8	2.3	2.8	1.97	Joint	
1603	1	7.9	8.2	7.8	7.97	Joint	
1644	2	5.3	5.7	6.4	5.80	Joint	
1685	1	3.5	3.6	4.4	3.83	Joint	
1726	1	3.5	4.2	4.6	4.10	Expansion Joint	
1736	1	4.9	4.8	4.9	4.87	Sealed Crack	
1769	2	1.7	3.6	4.3	3.20	Joint	

1808	1	3.1	5	5.4	4.50	Joint	
1849	4	4.8	5.3	5.1	5.07	Joint	Right wheelpath joint width = 0.5 in.
1856	6	1.7	2.2	1.5	1.80	Crack	
1896	0	4.7	5	5.6	5.10	Joint	
1931	7	3	2.6	4.4	3.33	Joint	
1972	8	6.3	5.8	5.7	5.93	Joint	
2013	11	4.4	4.2	3.9	4.17	Joint	
2026	3	-0.8	0	-0.1	-0.30	Sealed Crack	
2038	6	-0.6	-0.2	0.1	-0.23	Sealed Crack	
2055	0	23.4	9.5	4.8	12.57	Expansion Joint	Right wheelpath Joint width = 0.5 in. (Figure A.4 for Breaks)
2095	11	2.2	3.7	3.1	3.00	Joint	
2137	1	3	3.1	3.3	3.13	Joint	
2158	8	-1	-0.7	-0.2	-0.63	Sealed Crack	
2171	4					Station 408+00	
2178	5	4.4	5.2	6.3	5.30	Joint	
2219	6	1.5	2.6	2.5	2.20	Joint	
2267	1	1.6	2.3	2.6	2.17	Joint	Station 408+95

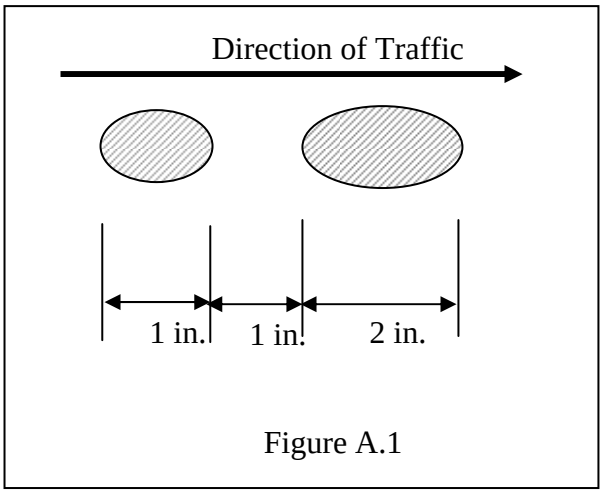

Figure A.1

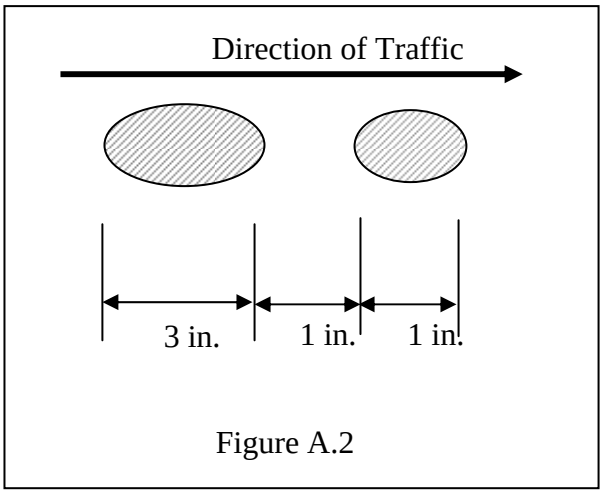

Figure A.2

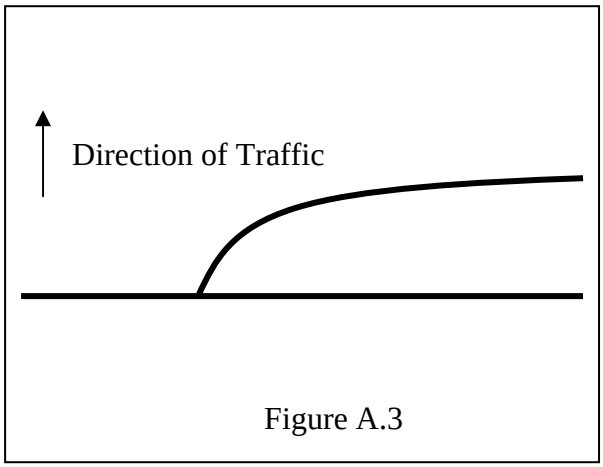

Figure A.3

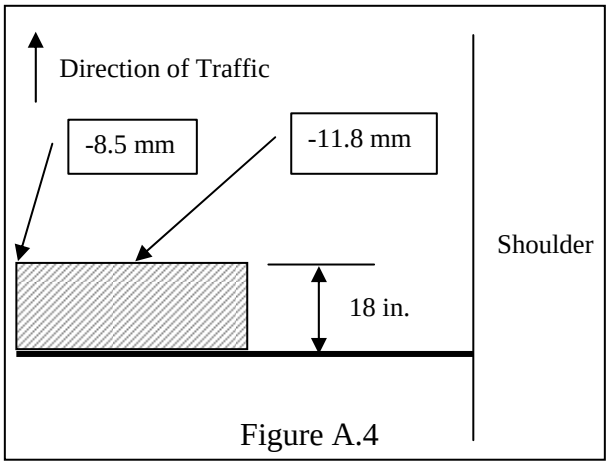

Figure A.4

SITE 2

Distance		Faulting (mm)			
Feet	Inches	Left	Center	Right	Comments
3	2				station 693+00
15	6	0.6		0.9	crack
44	1				joint
58	11	14.1		11	crack
69	10	-2.9		3	crack
85	9				joint
101	8	2.1		4.7	crack
126	6				joint
148	10	0.2		0.7	crack
167	8				joint
181	4	1.8		2.6	crack
209	3				joint
225	2	0.5		1.5	crack
251	0				joint
268	7	4.8		4.4	crack
276	9	-2.4		-1.8	crack
292	5				joint
307	11	2.4		7.2	crack
316	9	0.9		1.8	crack
334	0				joint
349	9	7.4		7.9	crack
363	10	-1.1		-1	crack
375	6				joint
399	10	3.3		4.5	crack
416	10				joint
431	11	0.2		2.3	sealed crack
444	2	-1.1		-0.5	sealed crack
458	7				joint
468	8	0.1		-0.5	sealed crack
477	1	-0.8		-0.6	sealed crack
487	10	1.6		3.2	wide sealed crack
505	0				joint

516	7	0.9		2.7	sealed crack
527	0	0.1		-1.1	sealed crack
541	4				joint
554	4	-0.5		-0.5	crack
571	0	1.2		13	sealed crack
582	10	0.6		-0.7	joint
605	8				station 699+00
624	4				joint
635	6	-1.7		0	sealed crack
644	9	-0.5		1.5	partial sealed crack
650	8	7		5.9	crack
664	11	-0.3		0.2	joint
676	9	-0.2		-0.4	sealed crack
704	6	-1		0.5	sealed crack
770	0				joint
758	1				joint
778	3	0.4		0.5	sealed crack
799	4				joint
812	8	6.5		10.6	sealed crack
820	1	0.2		-0.8	sealed crack
826	9	3.9		2.9	sealed crack
840	6				joint
858	2	3.5		4.5	sealed crack
867	1	-1.1		-0.3	sealed crack
882	1				joint
900	10	-1.1		1	sealed crack
911	8	0.8		-1.1	sealed crack
923	1	-0.3		-1	joint
942	10	1.8		2.2	sealed crack
953	4	-0.5		-1	sealed crack
963	5	-0.5		-0.4	joint
988	8	2.8		4.8	wide sealed crack
1004	8				joint
1024	3	-1.4		-1	sealed crack
1045	4				joint
1063	1	-0.5		-0.3	sealed crack

1075	11	-1		0	sealed crack
1086	5	-0.3		0	joint
1128	1				joint
1167	5	-0.3		-0.3	sealed crack
1169	4				joint
1210	0	0.5		1.2	joint
1251	5	0.4		0	joint
1274	11	1		-0.7	crack
1293	6				joint
1306	8	4.5		6.6	wide sealed crack
1334	8	1.8		0.7	joint
1343	5	0.4		0	sealed crack
1374	7	1.9		1.4	joint
1415	9				joint
1456	8				joint
1497	7				joint
1538	4				joint
1579	2				joint
1620	2				joint
1661	3				joint
1688	11	-1.2		0.2	sealed crack
1701	6	-0.1		0.3	joint
1732	10	0		0.3	sealed crack
1742	4				joint
1756	5	-0.8		1	sealed crack
1783	3				joint
1824	1				joint
1843	7	0.2		-0.5	sealed crack
1865	4				joint
1906	2				joint
1947	2				joint
1988	1				joint
2029	1				joint
2069	11	0.9		0.6	joint
2085	4	1.6		2.3	sealed crack
2096	11	5.3		4.6	sealed crack

2101	2	-0.1		2	sealed crack
2110	8	-0.3		0.4	joint
2151	3	0		-0.3	joint
2192	5	0.1		-0.6	joint
2233	0				joint
2274	0				joint
2315	0				joint
2356	0				joint
2397	0				joint
2438	0				joint
2479	0				joint
2506	3	0		-0.9	sealed crack
2520	0				joint
2561	0				joint
2572	8			-0.2	partial sealed crack
2602	0				joint
2616	9	-0.2		-0.9	sealed crack
2629	11	4.4		3.8	wide sealed crack
2643	0				joint
2684	0				joint
2720	1				station 720+00
2725	8				joint

24	4				error

SITE 3

Distance		Faulting (mm)			
Feet	Inches	Left	Center	Right	Comments
0	0				station 773+00 (core)
22	8				joint
32	9	4.6		8	crack
63	5				joint
87	4	-0.5		0	crack
104	4				joint
145	7				joint
186	4				joint
199	4	0.7		4.1	crack
227	2				joint
234	7	1.4		5.3	crack
258	8	1.6		4.3	crack
267	8				joint
300	6				station 776+00
309	4				joint
350	2				joint
362	4	1		3.3	crack
391	2				joint
432	3				joint
456	9	4		9.5	crack
465	0	1.6		1.6	crack
473	1				joint
488	2	0.6		1	crack
500	11				station 778+00
503	3	5.8		6	crack
514	1				joint
526	6	4.4		6.8	crack
554	11				joint
596	4				joint
636	11				joint
649	3	5.8		7	crack

656	4	3.2		3.3	crack
662	5	-1.6			crack
665	5			8	crack
672	2			-2.4	diagonal crack
678	2				joint
701	4				station 780+00
719	1				joint
747	9				mid-slab (8inch) deep>1inch
759	10	0.5		0.3	joint
790	10	-0.4		2	crack
800	10				joint + station 781+00
814	1	3.7		7.6	wide crack
822	10	0.8		-0.6	crack
841	11				joint
854	6	5.6		8.3	crack
882	10				joint
897	9	2.5		6	crack
923	10				joint
933	3	2.3		5.9	crack
945	0	8.3		9.6	crack
955	7	0.3		1.8	crack
964	9				joint
1001	7				station 783+00
1005	10				joint
1046	10				joint
1063	8	4.3		8	crack
1087	10				joint
1100	2	4.1		8.9	crack
1128	10				joint
1137	10	-0.3		0.7	crack
1143	7	3.5		6.3	crack
1153	6	-0.4		4.4	partial crack
1158	10	-1		-1.8	crack
1169	2				joint
1183	5	3.4		6.4	crack
1196	5	3.4		3.5	space wide crack

1202	3				station 785+00
1210	6	0.5		0	joint
1231	11	0		3.1	crack
1240	3	0.1		-1.4	crack
1251	8				joint
1292	11				joint
1302	4				station 786
1304	6	1.2		4.4	crack
1333	10				joint
1345	1	0.6		6.6	crack
1358	1	5.1		5.7	crack
1365	11	1.7		1.6	crack
1375	2				joint
1384	11	2		6.4	crack
1394	4	2.5		1.8	crack
1404	5	2.8		4.2	crack
1416	1				joint
1426	5	4.8		2.8	crack
1438	0	3.9		5.8	crack
1446	7	-0.2		-0.8	crack
1457	4				joint
1469	4	5.5		1.1	crack
1476	6	-0.5			crack
1478	9			-0.8	crack
1498	0				expansion joint
1510	2	1		3.2	crack
1540	1				joint
1581	0				joint
1595	2	-0.1		2.5	crack
1612	1	-1.8		-3.8	joint (patch)
1682	3				joint
1663	8				joint
1694	9	0.5		1	crack
1705	0				joint
1706	0				station 790+00
1712	0	-0.4		0.9	fault depth repaired joint

1732	1	-1.7		4	end of previous joint
1746	1	1		2.5	joint
1787	6				joint
1828	6				joint
1869	6				joint
1910	7				joint
1951	6				joint
1993	5				joint
2034	6	1.6		0.6	joint
2053	8	5.2		6.3	crack
2063	5	-0.4		0.3	spoiled crack
2076	3				joint
2094	6	0		0.8	crack
2116	8				joint
2158	2				joint
2199	3	-0.3		0.8	joint
2240	5				joint
2255	6	-0.2		0	crack
2281	8				joint
2297	8	3.1	3.7		crack
2323	0				joint
2364	3				joint
2379	0	1		2.1	crack
2405	4				joint
2408	8				station 797+00
2434	9	0		1.7	crack
2446	7				joint
2459	4	-0.5		-0.7	crack
2488	1				joint
2504	4	1.5		3.3	crack
2512	3	5.1		2.2	crack
2520	3	-1.5		-1.4	crack
2529	3				joint
2541	7	5.6		6.5	crack
2550	1	1.3		1.2	crack
2570	11	0.3		1	joint

2612	1				joint
2631	1	4.3		6	crack
2640	1	0.2		-0.3	crack
2653	3				joint
2694	7				joint
2712	1				(core) station (800+00)

12	0				error

SITE 4

Distance		Faulting (mm)			
Feet	Inches	Left	Center	Right	Comments
0	0				station 130+00
0	6	10		9.1	joint
57	1	1.9		1	repaired joint (patch)
110	4	2		4.3	repaired joint (patch)
166	4	0.7		2.5	spoiled crack (10" wide)
216	4	8.4		7.9	joint
266	1	5.4		4.9	wide crack
287	8	9.4		8.3	joint
323	1	0.5		0.4	spoiled crack (10" wide)
358	9	6.6		15.3	spoiled joint (4" wide)
				9	
399	4	3.5		7	patch joint
430	4	8.8		6.2	joint
445	7	2.9		5	spoiled crack (3" wide)
501	6				station 135+00
501	11	9.8		7.8	joint
523	8	-0.7		2.3	crack
573	7	6		5.2	joint
644	11	3.9		6.4	spoiled joint
665	7	4.5		6.5	repaired joint (patch)
716	4	8.1		7.1	joint
738	5	3.7		3.5	repaired joint (patch)
787	6	7.3		6.6	joint
837	2	4.3		4.9	spoiled crack
859	2	6.6		7.2	joint
930	10	4.1		5.7	joint
954	6	4.9		5.3	wide crack
1003	1	3.2		3.3	station 140+00
1045	5	1.6		1.2	patch joint
1073	8	7.2		5.4	joint
1106	9	3.7		2.8	crack
1119	8	3.2		4.3	crack

1145	6	10		8.5	joint
1166	1	1.1		5.5	repaired joint (patch)
1194	5	4.5		4.8	repaired joint (patch)
1217	1	10.8		7.7	joint
1235	11				start patch
1242	6				end of patch
1288	4	6.9		5.6	joint
1337	3				start patch
1343	10	-0.4		0.9	end of patch (repaired joint)
1381	9				start patch
1400	0	3.2		5.5	end patch (repaired patch)
1431	8	5.6		5.5	joint
1448	8	6.1		5	crack
1467	5	5.4		8.5	crack
1483	6				start patch
1490	2				end patch (repaired patch)
1520	10	6.7		5.7	wide crack
1546	6				start patch
1553	0				end patch
1575	0	8.2		8.4	joint
1593	5	0.3		0.8	crack
1611	10				start patch
1646	10	3.3		2	end patch (repaired joint)
1666	4	2.8		3.7	crack
1677	4	8		6.1	crack
1699	3	1.8		4.3	crack
1706	8				station147+00
1718	6	8		7.8	joint
1737	11	8		9.1	wide crack
1750	9	4.5		3.5	crack
1790	0	8.1		6.6	joint
1861	6	5.5		6.6	joint
1877	0				crack
1894	8	-10.8		-5.9	start patch
1920	4				end patch
1933	0	8.6		6.3	joint

1953	6				start patch
1960	1				end patch
1972	5				start patch
1986	9				end patch + start patch
1995	10				end patch
2004	8	9.7		9	joint
2019	7				start patch
2039	9				end
2053	4				start patch
2059	10				end
2075	9	13.8		10.7	joint
2092	1				start patch
2098	6				end
2118	3				start patch
2124	10	-0.6		0.3	end patch (repaired joint)
2147	4	8.9		6.7	joint
2167	7				start patch
2173	11				end
2189	0				crack
2195	10				crack
2208	3				station 152+00
2218	7	13.8		9.1	joint
2234	0				start patch
2240	11				end
2265	11	4.6		1.1	start patch
2272	6				end
2290	4	7.5		6.5	joint
2310	3	6.9		7.6	crack
2324	11				start patch
2344	5				end patch
2361	7	6.3		5	joint
2403	1	-2.6		-4.8	start patch
2420	11	6		3.1	end
2461	10				start patch
2468	6	0.9		1.6	end
2504	9	5.1		3.4	joint

2509	8				station 155+00
2532	2				start patch
2538	8	4.3		3.4	end
2557	3				start patch
2563	9	1.8		4.8	end patch
2576	4	12		10.9	joint
2627	6				start patch
2634	4	4.8		5.8	end
2647	8	9.1		7.1	joint
2667	1				start patch
2673	7	6		6.3	end patch
2682	3				start patch
2688	11	1.5		4.1	end
2697	6				start patch
2704	0				end
2710	7				station 157+00
2737	11	-0.8		-2.2	start patch
2752	11				end
2771	5				start patch
2778	0	-1.7		1.8	end
2791	0	8.1		10.9	joint
2858	11				start patch
2865	4	3		4.3	end
2892	1	4.6		5.3	crack
2933	8	9		10.5	joint
2967	3				crack
2975	6				start patch
2982	0	5.4		4.2	end
3005	1	5.7		4.5	joint
3011	6				station 160+00
3036	7	4.7		3.8	crack
3057	7				start patch
3064	1				end
3076	7	8		8	joint
3111	5				crack
3127	4	5.8		3.9	crack

3148	2	11		7.2	joint
3163	9				crack
3219	6	2.2		4.8	joint
3259	1	4.7		4.1	crack
3276	11	1.2		7.8	non measurable crack
				5	
3281	4	9.4		5.6	joint
3310	3				start patch
3316	11				end
3342	8	5.5		7.3	crack
3362	8	9.2		9.2	joint
3406	0	3.1		5.1	crack
3414	4				station 164+00
3434	7	7.3		8.2	joint
3485	1			4.6	diagonal crack
3487	5	5.1			
3506	7	9.5		10.5	joint
3519	4				crack
3536	5				start patch
3543	0				end
3556	8				start patch
3563	3				end
3599	8	3.3		4.7	crack
3619	4				start patch
3625	10				end
3636	6				crack
3649	2	9		7.1	joint
3720	5	10.9		10.5	joint
3791	11	9.8		8.9	joint
3815	7				crack +station 188+00
3827	10				crack
3847	4	1.7		4.5	crack
3863	4	9.9		9.1	joint
3874	1				crack
3884	10				start patch
3891	5				end

3915	9	2.1		2.1	crack +station 169+00
3948	2				start patch
3954	9				end
3966	5				start patch
3972	11				end
3986	11	6.2		4.2	crack
4021	5				start patch
4040	6				end
4077	7	7.5		8.6	joint
4116	11				station 171+00
4120	7	2.3		5.2	crack
4142	0				crack
4149	1	9.7		9.7	joint
4164	11				crack
4173	6	0.6		1.3	spoiled crack
4192	4				start patch
4203	6				end
4220	10	3.8		4.7	joint
4241	0				crack
4248	2	2.4			diagonal crack
4249	2			2.4	
4266	1				crack
4276	1				crack
4292	2	7		7.4	joint
4308	6	4.5		5.7	crack
4317	11				station 173+00
4326	11	5.2		6.9	crack
4363	10	10.5		10.3	joint
4375	4				crack
4389	5	8		8.8	crack
4400	0	7.7		8	crack
4418	7				station 174+00
4435	4	8		7.6	joint
4450	4	2.3		-1.7	start patch
4470	7	6		5.6	end
4490	0	7.5		7.8	crack

4506	10	9.2		10.3	joint
4524	11	6.8		25.8	spoiled crack
				18.5	

2	1				error

APPENDIX B: REPEATED MEASUREMENTS

SITE 2

Repeatability test

Distance		Faulting (mm)			
Feet	Inches	Left	Center	Right	Comments
650	8	7		5.9	crack

Direction		
traffic	transversal	repeated measure
6	5.1	5.9
6	5.9	5.5
5.8	6.3	5.7
5.9	6.3	5.8
5.1	5.5	5.8
		5.5
		5.7
		5.6
		5.7
		5.7
		5.5
		5.7
		5.8
		5.8
		5.6

interval (inch)	3	6	
average	5.76	5.82	5.686667
standard error	0.1144	0.2176	0.014489

SITE 3

Repeatability test (1)

Distance		Faulting (mm)			
Feet	Inches	Left	Center	Right	Comments
2541	7	5.6		6.5	crack

Direction		
traffic	transversal	repeated measure
7.7	6.8	7.1
7.1	7	7.2
6.8	6.8	7.1
7.1	7.1	7.1
6.9	6.5	7
	7.5	7
	7.4	7.1
		7
		7.2
		6.9
		6.9
		7
		7.2
		6.8
		7.1

interval (inch)	4	6	
average	7.12	7.014286	7.046667
standard error	0.0976	0.106939	0.013156

Repeatability test (2)

Distance		Faulting (mm)			
Feet	Inches	Left	Center	Right	Comments
1476	6	-0.5			crack

Direction		
traffic	transversal	repeated measure
-0.4	-0.3	-0.5
-0.4	-0.5	-0.5
-0.2	-0.2	-0.5
-0.7	-0.2	-0.6
-0.6	-0.7	-0.5
		-0.7
		-0.7
		-0.5
		-0.5
		-0.7
		-0.7
		-0.6
		-0.8
		-0.3
		-0.5

interval (inch)	4	6	
average	-0.46	-0.38	-0.57333
standard error	0.0304	0.0376	0.015289